Available online at www.sciencedirect.com
ScienceDirect
ELSEVIER
Palaeogeography, Palaeoclimatology, Palaeoecology 238 (2006) 125–150
PALAEO
www.elsevier.com/locate/palaeo

Calcareous nannofossil biostratigraphy and magnetostratigraphy of the Upper Miocene and Lower Pliocene of the Northern Aegean (Orphanic Gulf–Strimon Basin areas), Greece

E. Snel [a,*], M. Mărunțeanu [b,1], J.E. Meulenkamp [a,2]

[a] *Faculty of Earth Sciences, University of Utrecht, Budapestlaan 4, 3584 CD Utrecht, The Netherlands*
[b] *Geological Institute of Romania, Caransebeş Str. 1, RO-79678, Bucharest 32, Romania*

Received 25 November 2003; accepted 7 March 2006

Abstract

The transitional position of the Northern Aegean makes it an important area for studying the relation between the Mediterranean and the Eastern Paratethys. A chronostratigraphic framework has been obtained for the Late Neogene deposits along the Orphanic Gulf and in the Strimon Basin of Northern Greece by analysing calcareous nannofossil data and paleomagnetic results from eight sections. The local formations and major lithological units have been correlated with the Upper Miocene and Lower Pliocene stages. Furthermore, the obtained framework has facilitated a more detailed reconstruction of the effects of the Messinian salinity crisis on the sedimentary record.

Magnetostratigraphic data from the Strimon Basin result in an age estimate of 6.3 Ma for the Dafni–Choumnikon Formation transition, between normal polarity subchrons C3An.2n and C3An.1n. Since this Late Miocene age estimate corresponds closely to estimates of the Maeotian–Pontian boundary in the Eastern Paratethys (Dacic Basin), we believe this transition from marine to brackish conditions corresponds to this latter boundary. The gypsiferous unit in the basal part of the Choumnikon-equivalent beds along the Orphanic Gulf can then be correlated with the evaporites in the Northern Aegean and the Lower Evaporites of the Mediterranean Basin. Consequently, we assume that these Northern Aegean evaporites have been deposited between 5.96 and 5.59 Ma.

Freshwater deposits above the evaporites are easily traceable across the Orphanic Gulf area, as a gravel or sandstone unit topped by a travertine marker bed, and have a wide lateral continuation. Since their position is intermediate between the shallow marine gypsum/anhydrite and the more open marine clastics of the Pliocene, we argue that these beds correlate with the desiccation phase of the Mediterranean and Black Sea basins. This intra-Messinian event probably occurred between 5.59 and 5.50 Ma, thus predating the Upper Evaporites or Lago Mare of the Mediterranean.

A clear recognition of the Miocene–Pliocene boundary remains problematic in the Orphanic Gulf area. Nannofossil assemblages in the sections suggest a higher position of the local base of the Pliocene than indicated by the level with the first appearance of planktonic and benthic foraminifera. Discontinuous occurrences of levels containing nannofossil assemblages of Zone MNN11b–c are found between the travertine unit and the lowermost Pliocene beds, representing brief marine ingressions. The latter show that in the latest Messinian, (presumably) temporary connections of Atlantic/Mediterranean waters with the Northern Aegean Basin existed. These marine ingressions likely extended further into the Eastern Paratethys, as demonstrated by

* Corresponding author. Tel.: +31 30 253 5125; fax: +31 30 253 3486.
E-mail addresses: snel@geo.uu.nl (E. Snel), mariana.marunteanu@yahoo.com (M. Mărunțeanu), meulenkamp@nioz.nl (J.E. Meulenkamp).
[1] Fax: +31 222 319674.
[2] Fax: +31 30 253 2648.

0031-0182/$ - see front matter
doi:10.1016/j.palaeo.2006.03.022

the presence of nannofossil assemblages in the Middle and Upper Pontian of the Dacic and Euxinic Basins. The events around the Miocene–Pliocene transition resulted in a fairly abrupt change from brackish to open marine conditions in a relative deep basin, which was subject to increased rates of subsidence from the onset of evaporite deposition in the Late Messinian onward.

Keywords: Biostratigraphy; Calcareous nannofossils; Paleomagnetism; Northern Greece; Messinian; Neogene

1. Introduction

During the Late Neogene, the connection between the Atlantic Ocean and the Paratethys via the Mediterranean Sea was restricted and periodically interrupted. This prevents straightforward bio- and chronostratigraphic correlations between the Mediterranean and the Paratethys realms. Marine and brackish faunas in the Miocene and Pliocene successions of the Northern Aegean (the Orphanic Gulf area and the Strimon Basin in Northern Greece; Fig. 1) show the influence of both the Mediterranean and the Paratethys realm on the palaeoenvironment of this sedimentary domain (Gramann and Kockel, 1969; Papp and Steininger, 1979; Steffens et al., 1979; Stevanoviæ, 1990; Syrides, 1998; Popov and Nevesskaya, 2000). Apparently, this part of the Northern Aegean served as an intermediate basin linking both water masses. Therefore, the Orphanic Gulf–Strimon Basin area is a key area for studies of aquatic connections and faunal exchanges between the Mediterranean and the Paratethys.

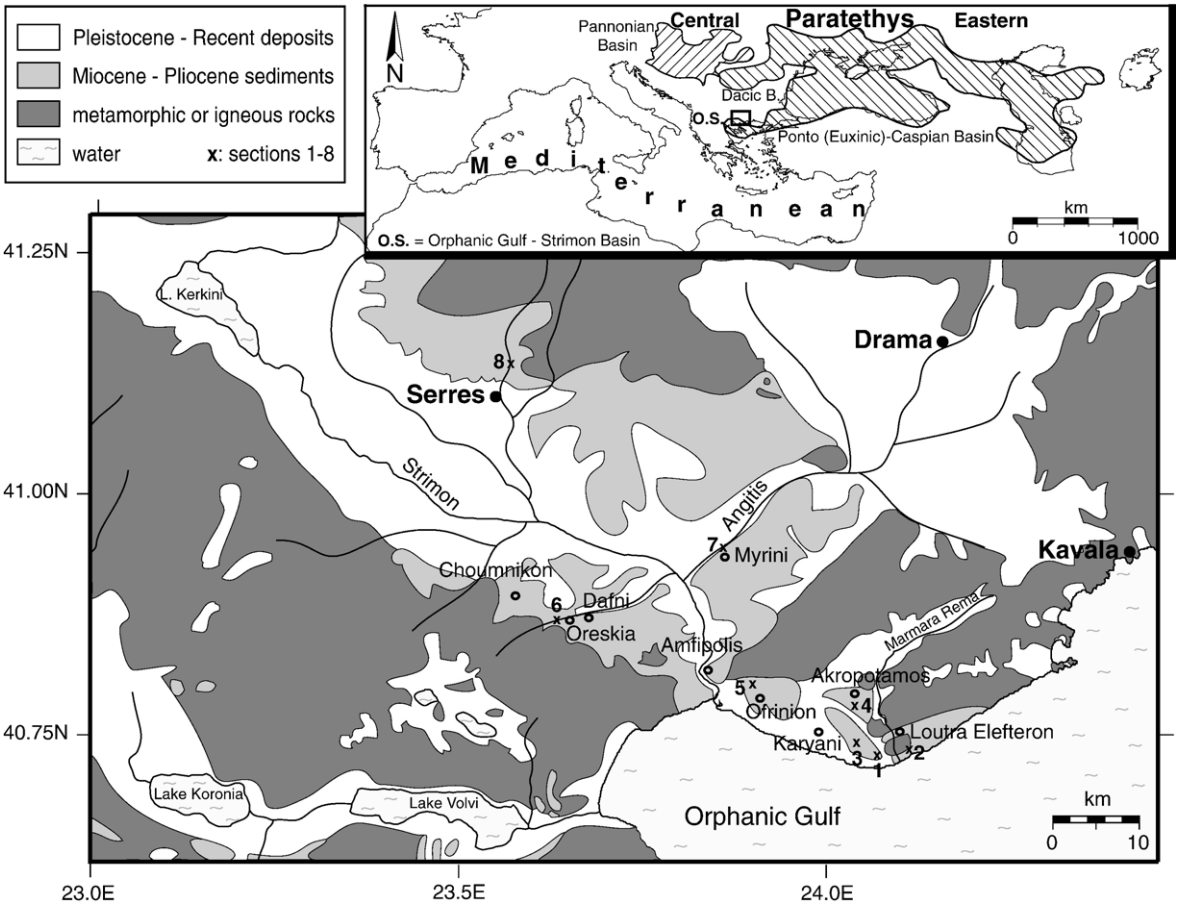

Fig. 1. Simplified geological map of the Orphanic Gulf and Strimon Basin areas (after Bornovas and Rondogianni-Tsiambaou, 1983) showing the locations of sections Kavala Road West (1), Kavala Road East (2), "Rema Marmara" (3), Akropotamos (4), Ofrinion (5), Eziovis Rema (6), Myrini (7) and Labyrinthos (8). Inset map shows the palaeogeography of the Paratethys region during the Late Miocene, superimposed on present-day geography, with location of the Orphanic Gulf–Strimon Basin. Modified after Steininger and Papp (1979).

The relation of observed evaporites, i.e. the gypsum of the Orphanic Gulf area (Meulenkamp, 1979) and anhydrite with halite found in offshore drillings near the island of Thasos (Pollak, 1979; Proedrou, 1979), with the Messinian salinity crisis is not clearly demonstrated (Rögl et al., 1991), because of inaccurate dating of these deposits. Furthermore, the effect and timing of the desiccation event in the Mediterranean and Black Sea basins is still subject of debate (Clauzon et al., 1996; Krijgsman et al., 1999; Roveri et al., 2001; Clauzon et al., 2005).

This study aims to provide an age model for the various sections and outcrops within the Orphanic Gulf–Strimon Basin area by correlating these with the sequence of Mediterranean and Paratethys stages. For this purpose, several sections in the coastal area of the Orphanic Gulf and on both sides of the river Strimon have been sampled. The calcareous nannofossil content of all sections has been analysed qualitatively; from two sections a magnetic polarity record was obtained. The resulting chronostratigraphic framework will be used to link bio- and lithostratigraphic observations from the Orphanic Gulf area and the Strimon Basin with events in the Mediterranean and the Eastern Paratethys.

2. Geological setting and stratigraphy

The contours of the present-day Orphanic Gulf–Strimon Basin area (Fig. 1) were formed during the Late Pliocene in response to strike-slip movements in the North Aegean trough, along a splay of the North Anatolian Fault (Dinter and Royden, 1993; Dinter, 1998). This relatively recent extensional deformation resulted in a series of North Aegean basins with Late Pliocene and younger infill and was superimposed on the effects of extension along a shear zone at the northern margin of the Aegean Sea during the Middle Miocene to Early Pliocene. This earlier deformation, on a larger scale related to extension in the back-arc of the Hellenic subduction zone, created the accommodation space for the older Neogene sediments. For reasons of convenience, the terms Orphanic Gulf and Strimon Basin are used, rather than the various (local) names for the presently peripheral basins in these areas, such as the Akropotamos, Pieria and Strymonikos basins, or the Angitis and Serres basins, respectively (Psilovikos and Syrides, 1983; Karistineos and Georgiades-Dikeoulia, 1986; Dermitzakis et al., 1986).

Miocene and Pliocene deposits are exposed on both sides of the river Strimon and east of its mouth along the

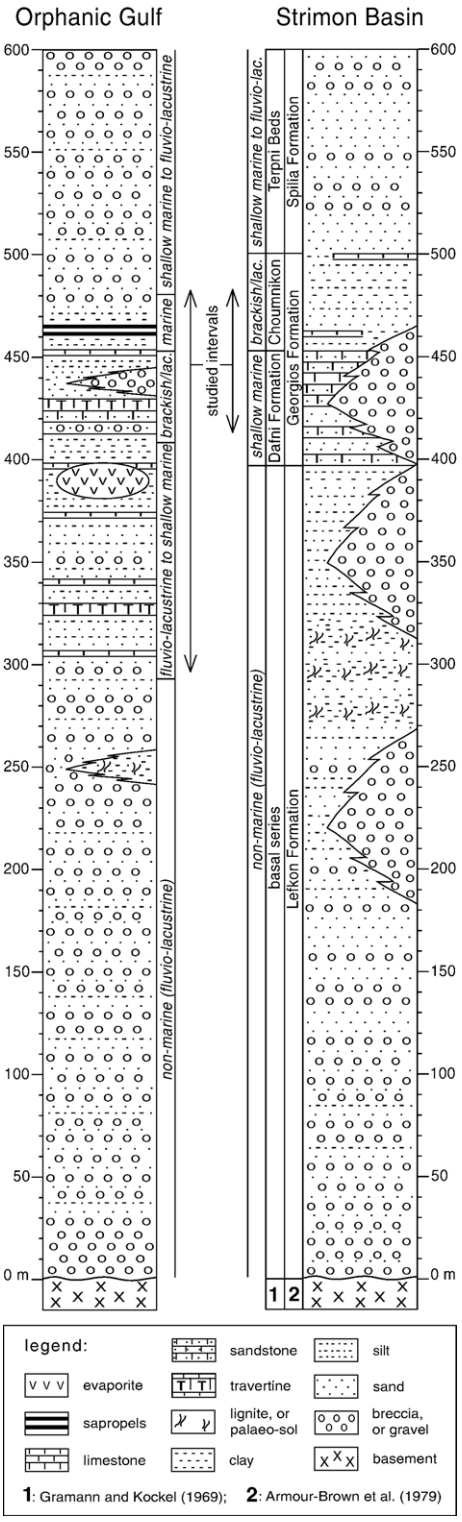

Fig. 2. Composite stratigraphic columns and interpretation in terms of general depositional environments for the Neogene of the Orphanic Gulf and Strimon Basin areas. Modified after Gramann and Kockel (1969), Armour-Brown et al. (1979), Steffens et al. (1979), Psilovikos and Syrides (1983), and Popov and Nevesskaya (2000).

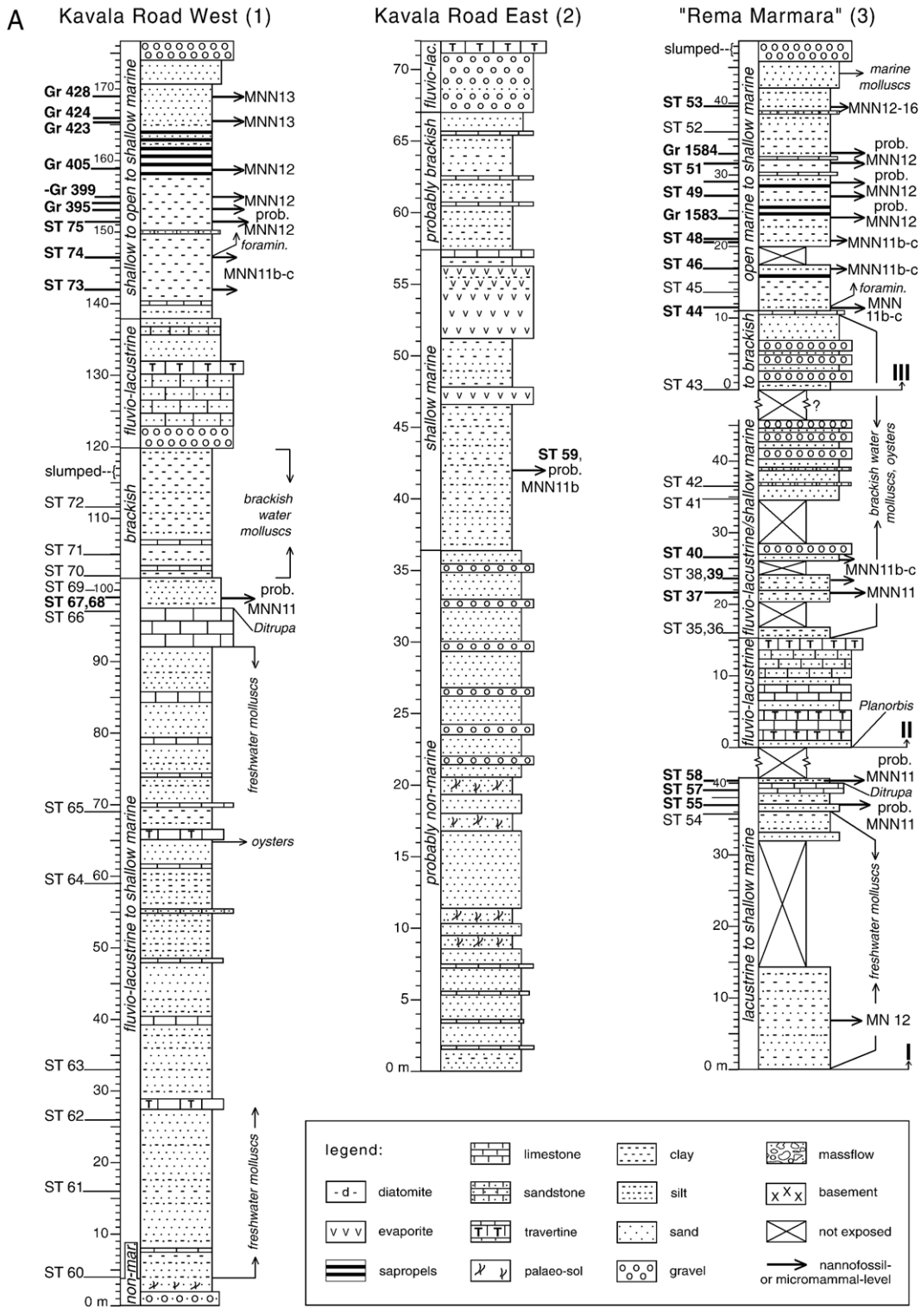

Fig. 3. Lithology, depositional environment, position of samples, fossil content and calcareous nannofossil zonal assignments of the (composite) sections of (A): Kavala Road West (1), Kavala Road East (2), "Rema Marmara" (3), and (B): Akropotamos (4), Ofrinion (5) and Eziovis Rema (6). Sections (1) and (3) are based on Steffens et al. (1979) and on our own observations; Section (4): modified after Dermitzakis et al. (1986) and based on Steffens et al. (1979) and on our own observations; Section (6): based on Gramann and Kockel (1969) and on our own observations. Levels with calcareous nannofossils are indicated by bold sample codes and arrows with interpreted MNN-zone.

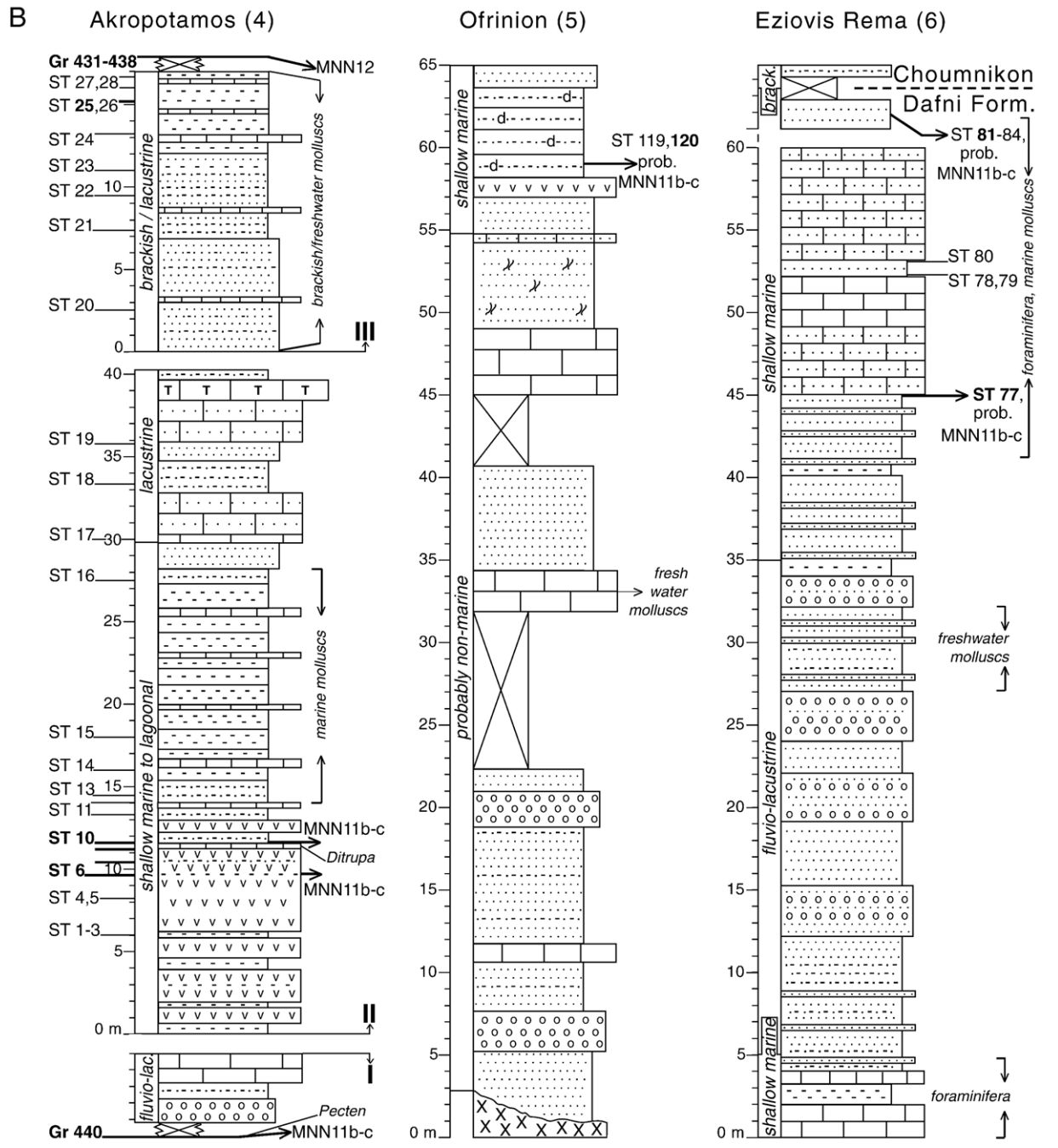

Fig. 3 (*continued*).

Orphanic Gulf coast (Fig. 1). In the latter area, approximately 300 m of fluvio-lacustrine conglomerates, sands and occasionally clays with lignite intercalations constitute the lower part of the Neogene sequence (Fig. 2). They are followed by alternating clastics and carbonates, reflecting lacustrine, brackish water, or shallow marine conditions. In the relatively open marine sandy or silty clays above (370–410 m), locally lenticular gypsum bodies occur, which underlie lacustrine and brackish beds containing Pontian age ostracodes (Meulenkamp, 1979; Steffens et al., 1979). These well-bedded strata are covered by a conglomerate or sandstone unit, with on top freshwater limestones and travertines, followed by brackish water clastics. The

overlying open marine clastics and sapropel–marl alternations (from 450 m upwards) were reported to be of earliest Pliocene age (Steffens et al., 1979). Finally, uplifted shallow marine sands and gravels of the last, Upper Pliocene–Pleistocene, marine series in the Orphanic Gulf area unconformably cover the tilted and disrupted sediments of the previous, Upper Miocene–Lower Pliocene marine cycle (Psilovikos and Syrides, 1983; Dinter and Royden, 1993).

The sequences of coarse clastics exposed along the river Strimon and near the city of Serres, resemble those of the Orphanic Gulf area. They pass upwards into sands and clayey lignites, locally interrupted by conglomerates and breccias of basement rocks, and are collectively referred to as basal series or Lefkon Formation (Gramann and Kockel, 1969; Armour-Brown et al., 1979; Fig. 2). The oldest marine beds above this fluvio-lacustrine basal part constitute the Dafni Formation. This marine unit, containing sands, sandstones and (coral) limestones, has been regarded by these authors to be the equivalent of sediments of the Eastern Paratethys assignable to the Maeotian. The overlying Choumnikon beds are mainly brackish water sand, silt and clay deposits, which contain mollusc and ostracod associations of (Early) Pontian age. In the northern part of the basin, near Serres, these marine and brackish successions (Georgios Formation of Armour-Brown et al., 1979) contain granite breccia interbeds. There, these (partly) tilted and folded Upper Miocene beds are unconformably covered by Lower Pliocene fluvio-lacustrine, locally shallow marine (Popov and Nevesskaya, 2000), sand and gravel successions of the Spilia Formation. The Terpni beds comprise the equivalent of this formation along the river Strimon.

3. Sections and sampling

A selection of the sections described by Gramann and Kockel (1969) and Armour-Brown et al. (1979), in the Strimon Basin, and of those described by Steffens et al. (1979), Psilovikos and Syrides (1983) and Syrides (1998), in the Orphanic Gulf area, was sampled for this study. Many localities, especially the sites documented by Gramann and Kockel (1969), were severely weathered or overgrown with vegetation. The eight sections that yielded (age-diagnostic) calcareous nannofossils, or conclusive paleomagnetic results, will be presented here.

3.1. Kavala Road West

Steffens et al. (1979) recorded a section along the north side of the coastal highway Thessaloniki–Kavala (E90), under construction at that time, between the mouth of the river Strimon and the town of Kavala. The exact location is 5 km east of the Karyani village traffic lights, 3 km east of section "Rema Marmara", 4 km west of the Marmara Rema-bridge (at the turn-off to Loutra Elefteron) and 5.5 km west of section Kavala Road East (Section 1; Fig. 1). Outcrops along the road are presently limited to 50 m of the lower 100 m of the original section. On the hill slopes within 100 m off the road, more and fresher outcrops are exposed. Overlying a series of sands and conglomerates, they constitute a continuous section of approximately 177 m (Fig. 3A). The lower 90 m consist of conglomerates and red, sandy palaeo-sols at the base, followed by fluvio-lacustrine sands, clays, limestones and travertinous limestones (samples ST 60–65), containing many levels with freshwater molluscs and ostracodes. One bed with oysters (at 65 m) indicates that occasionally brackish to shallow marine conditions occurred. Marine influence is supported by the presence of *Scaphopoda* and *Ditrupa* in a thick calcareous bed at 97 m (sample ST 66). Also the overlying finely bedded silts and sands contain fragments of these invertebrates (samples ST 67–69). The limestone forms an east facing dip-slope, extending towards the top of the still existing outcrops along the road. Samples 70–72 were taken from an 18 m thick succession of laminated silts and clays, containing brackish water molluscs, which are, in the lower part of the succession, alternating with platy limestones. In the upper part, the silts and clays are folded because of slumping. On top lies a massive conglomerate-, sandstone- and travertine bed forming a second dip-slope, which is also exposed in the base of the next hill to the east. This non-marine bed is covered by 6 m of partially calcified sands, followed by 36 m of marine clayey marls that alternate with a few sandy limestone beds and a regular series of sapropels. Of samples ST 73–75, recovered from the lower part of these marls, ST 74 and especially ST 75 contain abundant benthic and planktonic foraminifera (without index species, however). The marls, grading upward into sands, end with a gravel deposit. These uppermost 45 m of the present-day section, constituting the lower part of a previously excellently exposed sequence, were sampled by Steffens et al. (1979; samples Gr 395–430) during road construction and interpreted as Lower Pliocene.

3.2. Kavala Road East

At km 124 along the same road to Kavala, 5.5 km east of section Kavala Road West, a 72 m thick, predominantly sandy section with gypsum/anhydrite

was recorded on the northern side (Section 2; Figs. 1 and 3A). The upper half of the succession is also partly exposed in less weathered outcrops along the track towards the beach below the road. Intercalated between 9 and 21 m in the well-bedded sands, limestones and conglomerates, are four sandy palaeo-sols, indicative of non-marine conditions. Sample ST 59 was taken from laminated clays and sands below the first gypsum bed in an outcrop below the south side of the road. Eastward, along the beach, the sequence ends with conglomerate beds and travertine deposits on top.

3.3. "Rema Marmara"

This is a misleading name (Steffens et al., 1979; De Bruijn, 1989) for the discontinuous section exposed along a gravel road on the bed of a small, unnamed stream, south of the village of Akropotamos and 7 km west of the bridge over the real Marmara Rema (Section 3; Fig. 1). Neogene deposits of several hundreds of metres, including a basal conglomerate series overlying the granite basement, are at present only partly exposed. A composite section, showing three exposed intervals (subsections I, II and III; Fig. 3A), was recorded above the conglomerates. The lower subsection (I), 1 km north from the main road to Kavala, consists of 15 m of lacustrine clays and sands with mollusc lags. In these beds, De Bruijn (1989) found a small rodent fauna suggesting a Middle Turolian age (MN 12), which is approximately time-equivalent with the Late Tortonian (about 8 to 7 Ma: Steininger et al., 1996). After an unexposed interval of 18 m, the succession continues with 6 m of sands and marls, containing *Unio* fragments and a 3 m thick *Ditrupa*-bearing shallow marine sand and carbonate bed at the top (samples ST 54–58). These beds are strongly sheared due to extensional block rotations (Dinter, 1998). Beyond a water basin, 250 m upstream, subsection II is exposed. The variable orientation of the bedding and the many faults hamper a reliable estimation of the thickness of the unexposed beds between subsections I and II. Outcrops in the lower part of subsection II consist of 15 m of sandstone and travertine with sand intercalations and a lag-deposit with *Planorbis* at the base. In scattered outcrops of the overlying laminated sandy clays, samples ST 35–39 were collected along a right tributary of the dry stream. Samples ST 40–42 were taken from a 20 m thick sand and conglomerate unit in the uppermost outcrops in this side valley. The well-bedded sands, alternating with sandstones and silts, contain a few levels with brackish water molluscs and oysters.

Sampling was continued in subsection III along the main stream. Approximately 150 m upstream of the calcareous base of subsection II, a 10 m thick sand and gravel series covering the first silty clay bed (sample ST 43), is encountered on the western side of the valley. Directly above this coarse clastic unit, further up the slope, a thin limestone bed underlies 8 m of silts and clays with rich and diversified benthic and planktonic foraminiferal associations (samples ST 44–46). Samples ST 47–53 were collected from a 20 m thick series of thin-bedded silts and clays, alternating with sapropels, limestones, sands and sandstones exposed 100 m upstream on the bottom of the valley. Steffens et al. (1979) described the strata from the same interval (samples Gr 1583–1585), presented here as subsection III, and interpreted them as a series of brackish beds containing ostracodes indicative of the Pontian, immediately followed by open marine clays with Early Pliocene foraminifera. Succession III ends with a coarsening upward sand and gravel unit, showing metre-scale slumps near the top. The position of the top of subsection II with respect to the base of subsection III is unclear, but the lithological differences between the two units exclude the probability of an overlap of more than ten metres.

3.4. Akropotamos

South of this village, several outcrops of Neogene sediments can be observed (Section 4; Fig. 1). These sediments unconformably overlie the faulted limestone basement. The strata are often severely disturbed by normal faulting (Dinter, 1998), thereby preventing the recording of a long continuous section. Steffens et al. (1979) described hundreds of metres of fluviatile to shallow marine fine-grained clastics and conglomerates in the basal part of the Neogene. Thin-bedded clays and sands also contain leaf and fish fossils, while in the uppermost part oysters, *Pecten* and calcareous nannofossils belonging to Zone NN11 or higher occur (Steffens et al., 1979). In a small outcrop above this marine level (sample Gr 440), the top of the basal subsection (I) is presently represented by 5 m of conglomerate, silt and limestone (Fig. 3B). These beds are overlain by a second, 40 m thick subsection (II), which is exposed in an adjacent, new quarry 1.5 km south of the village. It consists of gypsum, with on top a calcareous bed containing *Ditrupa*, limestone beds and silty clays with sandstones and travertine deposits in the uppermost part. Samples ST 1–19 have been taken from a laterally identical succession, in an old quarry 500 m to the

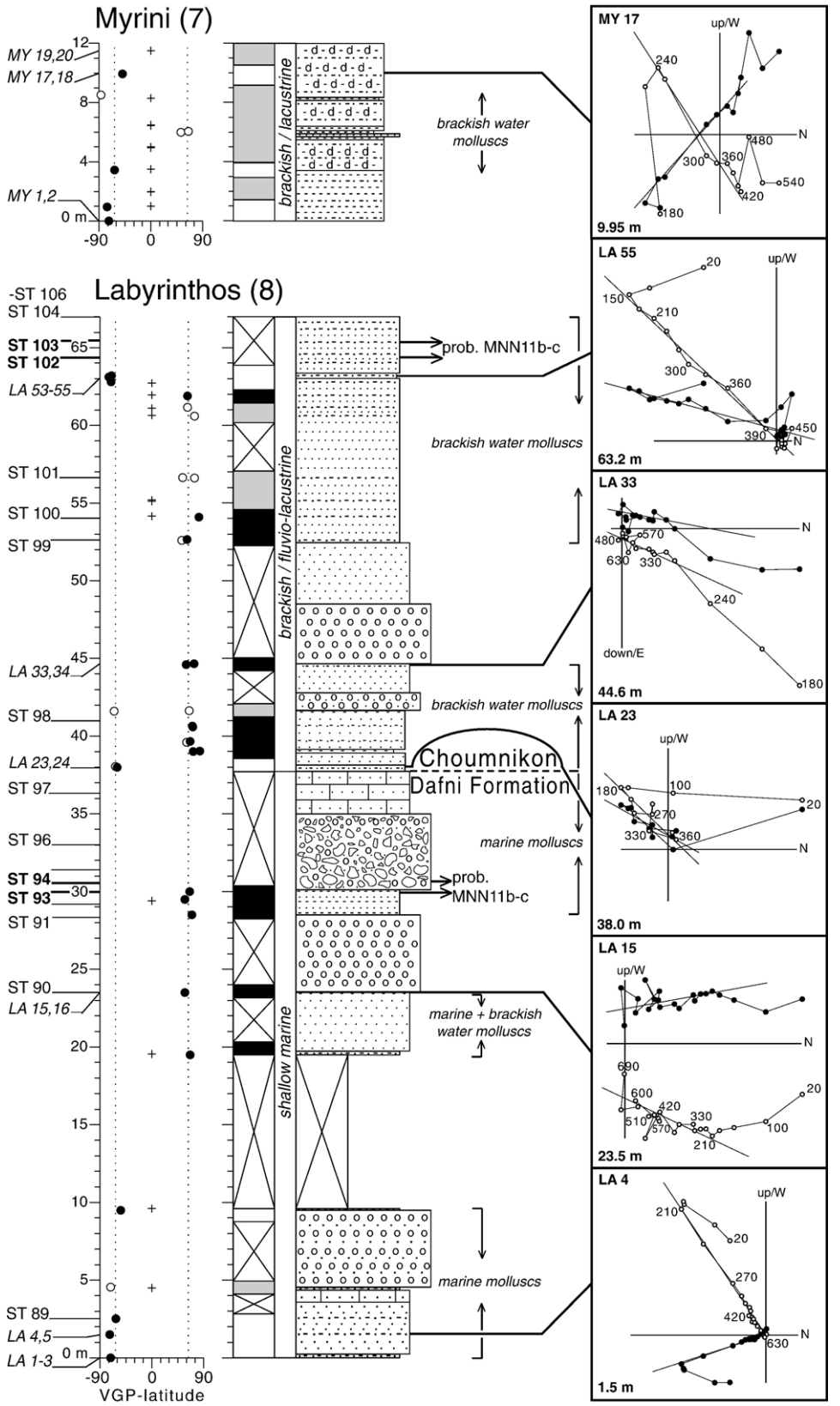
Myrini (7)
MY 19,20
MY 17,18
MY 1,2
0 m
-90
0
90
brackish / lacustrine
brackish water molluscs
MY 17
up/W
240
N
480
300
360
540
420
180
9.95 m
Labyrinthos (8)
-ST 106
ST 104
ST 103
ST 102
LA 53-55
ST 101
ST 100
ST 99
LA 33,34
ST 98
LA 23,24
ST 97
ST 96
ST 94
ST 93
ST 91
ST 90
LA 15,16
ST 89
LA 4,5
LA 1-3
VGP-latitude
brackish / fluvio-lacustrine
prob. MNN11b-c
brackish water molluscs
Choumnikon
Dafni Formation
marine molluscs
prob.
MNN11b-c
shallow marine
marine + brackish
water molluscs
marine molluscs
LA 55
20
150
210
300
360
450
390
63.2 m
LA 33
570
480
630
330
240
down/E
180
44.6 m
LA 23
100
180
270
330
360
38.0 m
LA 15
690
600
420
510
570
330
210
100
23.5 m
LA 4
210
270
420
630
1.5 m

northeast. Dermitzakis et al. (1986) studied marine bivalves and lagoonal fish remains from the beds above the evaporites and correlated subsection II of section Akropotamos with the Messinian. Above the sandstone and travertine beds, samples ST 20–28 from a third, 61 m thick subsection (III, of which only the well-exposed lower 17 m are shown in Fig. 3B) of alternating laminated fluvio-lacustrine clays, silts, sands and limestones contain brackish and freshwater ostracodes and molluscs. Calcareous nannofossils, belonging to Zone NN12 and indicating an Early Pliocene age, were reported by Steffens et al. (1979) from still younger, marine clastic units closer to the village (samples Gr 431–438). These beds are at present poorly exposed.

3.5. Ofrinion

Other scattered outcrops of gypsum are found north of the village of Ofrinion (or Ophrynio; Psilovikos and Syrides, 1983), near the margin of the basin (Section 5; Fig. 1). There, the lower part of the poorly exposed Neogene succession is separated from the crystalline basement by normal faults. The succession, presented as an idealized section of at least 65 m (Fig. 3B), consists of a probably non-marine part with conglomerate, sand, (travertinous) limestone beds and sandy palaeo-sols, followed upwards by a shallow marine part with gypsum/anhydrite and laminated, diatomaceous limestones, alternating with thin clay and sand beds (samples ST 119 and 120) and overlain by sands.

3.6. Eziovis Rema

West of Oreskia, Gramann and Kockel (1969; their profile 4) recorded a section in the Dafni beds on the northern bank of this stream (Section 6; Figs. 1 and 3B). They described a succession of 60 m of marine sands and sandy limestones (samples ST 77–80), with a non-marine clastic intercalation between 5 and 35 m. On top of the southern bank of the stream, near the village entrance, two metres of sands with *Pecten* and oysters are exposed (samples ST 81–84). These beds represent the uppermost part of the Dafni Formation, and are followed by brackish marls and sands of the Choumnikon beds.

3.7. Myrini

A new quarry, 1 km north of this village, is situated at the location of profile 62 of Gramann and Kockel (1969) on the south side of the bridge of the Serres–Amfipolis road across the river Angitis (Section 7; Fig. 1). In the quarry at the foot of a hill, a section of 12 m with diatomaceous clays and silts was recorded (Fig. 4). These sediments form a part of the Choumnikon Formation (Gramann and Kockel, 1969) and are rich in brackish water molluscs, ostracodes, diatoms and fish remains. On top of the hill, 20 m above the rear wall of the quarry, the laminated brackish water deposits are unconformably overlain by shallow marine gravels and sands with *Pecten* and oysters, still attached to the limestone cobbles (pers. comm. G. Syrides, 2000). The beds of the Choumnikon Formation, dipping 15° SE, are intersected by listric normal faults. Samples MY 1–20, for magnetostratigraphy, were taken every 1–2 m.

3.8. Labyrinthos

A section in this valley northeast of Serres (Section 8; Fig. 1) was recorded by Gramann and Kockel (1969; profile 31) and revisited by Karistineos and Georgiades-Dikeoulia (1986), by Syrides (1998: Perdikari locality) and by Popov and Nevesskaya (2000). The record originally documented by Gramann and Kockel measured 170 m, including an unexposed interval between 70 and 140 m. Their section covered marine sands, sandy limestones and gravels of the Dafni beds, followed by brackish clays, sands and (in the lower part) gravel beds of the Choumnikon Formation which contain ostracodes and molluscs characteristic of the Pontian. Popov and Nevesskaya

Fig. 4. Magnetostratigraphy of sections Myrini (7) and Labyrinthos (8), Strimon Basin. Lithology, mollusc content, depositional environment, paleomagnetic results, interpreted polarity zones, and thermal demagnetization diagrams of selected samples. For legend: see Fig. 3; stratigraphy and mollusc content of the schematic section Labyrinthos are based on Gramann and Kockel (1969), on Popov and Nevesskaya (2000) and on our own observations. Paleomagnetic results (from samples LA 1–55 and MY 1–20) are interpreted as virtual geomagnetic polar (VGP) latitude. Closed (open) circles denote (less) reliable ChRM directions; plusses are used for inconclusive results. In the polarity column black (white) denotes normal (reversed) polarity, grey indicates undetermined polarity; crossed intervals are used for those parts of the section where no samples were taken. Demagnetization diagrams denote orthogonal projections of NRM vector end-points, after tectonic correction, with open (closed) symbols on the vertical (horizontal) plane; values represent temperature increments in °C; best-fit lines indicate interpreted polarity directions. Stratigraphic levels and sample numbers are in the lower and upper left corners, respectively. Levels with calcareous nannofossils are indicated by bold sample codes and arrows with interpreted MNN-zone.

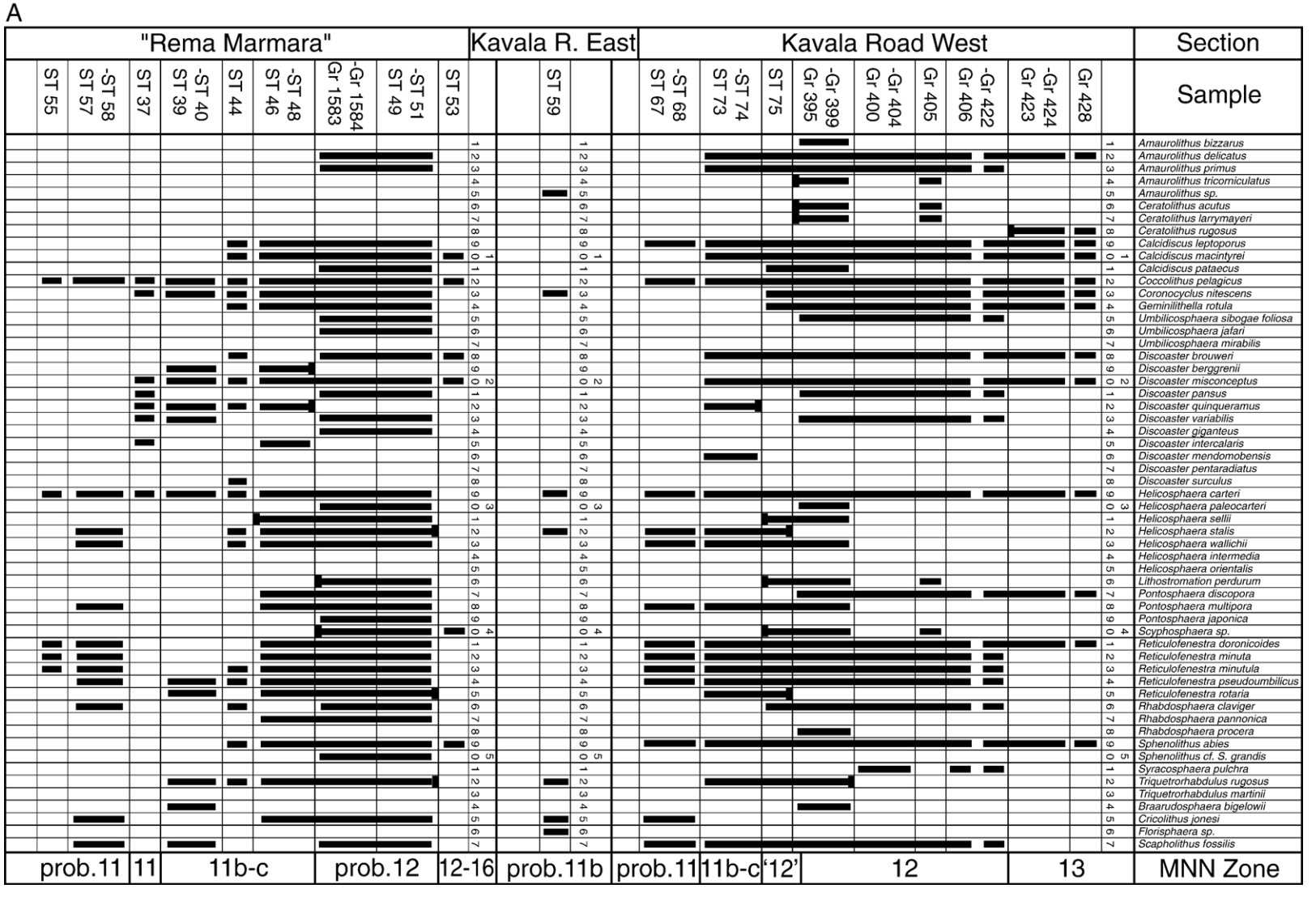

Fig. 5. Species distribution per sampling interval in sections Kavala Road West, Kavala Road East, "Rema Marmara" (A), and in sections Akropotamos, Ofrinion, Eziovis Rema and Labyrinthos (B). Zonal assignments of the sampling intervals, according to the biozonation of Raffi and Rio (1979), are indicated on the right side. Only samples yielding nannofossils are listed (see Figs. 3 and 4).

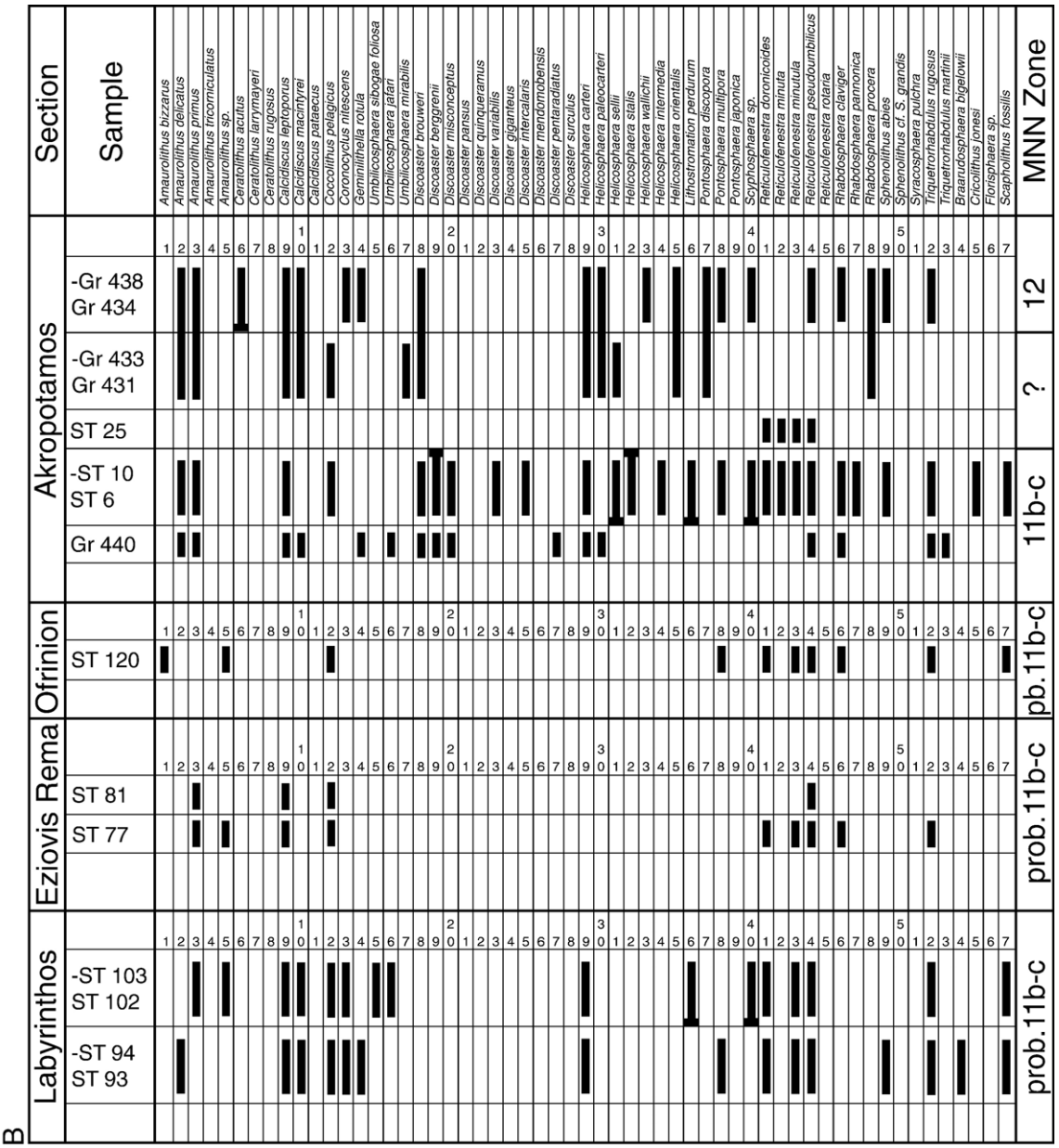

Fig. 5 (*continued*).

(2000) included the overlying Pliocene Spilia Formation in their study of the Neogene. This unit starts with marine clays including oysters, followed by fluvio-lacustrine sands and conglomerates. Unlike Popov and Nevesskaya (2000), who adopted the older subdivision of Dafni and Choumnikon Formation, Karistineos and Georgiades-Dikeoulia (1986) correlated the generically equivalent Georgios Formation with the sediments supposed to reflect the Early Pliocene transgression. This interpretation was based on the presence of *Pecten benedictus* in the middle part of the Georgios Formation (or the top of the Dafni beds) in section Labyrinthos.

The 30–36° NE-dipping beds of section Labyrinthos were sampled for bio- and magnetostratigraphy (Fig. 4; samples ST 89–106; LA 1–55). The basal and middle parts of the Dafni Formation, as well as the interval straddling the Choumnikon–Spilia transition (not shown), are poorly exposed at present and were not sampled. In addition, the interval containing the Dafni–Choumnikon transition is poorly visible, making the field determination of its exact position uncertain. The position of this last formation boundary was therefore adopted from Gramann and Kockel (1969).

4. Magnetostratigraphy

4.1. Method

Two oriented cores per sample level were taken with a water-cooled, generator-powered electric drill and oriented with respect to the present-day north with a magnetic compass. The samples from the fresh-cut sediment surface were sawn into ~ 10.5 cm^3 specimens at the laboratory.

The natural remanent magnetization (NRM) of the specimens was thermally demagnetized by progressive heating in a magnetically shielded, laboratory-built furnace with temperature steps of 30–50 °C, up to a maximum of 700 °C. At least one specimen per sample level was measured on a 2G Enterprises horizontal DC SQUID magnetometer to obtain a magnetic polarity record.

4.2. Results

The samples from section Kavala Road West, taken from levels between 135 and 165 m, and those recovered from subsection III of section "Rema Marmara" appeared to be strongly weathered and proved useless for magnetostratigraphic interpretations. In sections Myrini and Labyrinthos thermal demagnetization diagrams (Zijderveld, 1967) yielded in general straightforward results (Fig. 4). In a number of specimens, low-temperature components, often parallel to the direction of the present-day field before bedding plane correction, were removed at 100–240 °C (e.g. samples LA 4, 23 and 55; Fig. 4). These were considered to be secondary signals, either laboratory-induced or recent overprints caused by weathering. Both normal and reversed magnetic field components, interpreted as primary, characteristic remanent magnetization (ChRM) directions, were gradually removed at higher temperatures, varying from 360 to over 600 °C. Specimens from section Myrini and from the upper 10 m of section Labyrinthos gave occasionally inconclusive results. The ChRM was determined by best-fit lines through the NRM vector end-points for a representative temperature interval.

The results are presented in two polarity columns (Fig. 4). Despite the fresh outcrops of clays and silts in the quarry of Myrini, only four levels yielded useful magnetic results. Counter-clockwise rotation, probably associated with listric faulting, affected the reversed polarity signal considerably (sample MY 17). A

Plate I. Calcareous nannofossils from section Kavala Road West, Orphanic Gulf area

1). *Amaurolithus delicatus* Gartner and Bukry, ×1600; sample ST 73. Parallel light.
2). *Discoaster quinqueramus* Gartner, ×2000; sample ST 74. Parallel light.
3). *Discoaster quinqueramus* Gartner, ×3100; sample ST 74. Parallel light.
4–5). *Discoaster misconceptus* Theodoridis, ×2900; sample ST 74. (4) Parallel light; (5) crossed nicols.
6). *Amaurolithus delicatus* Gartner and Bukry, ×1700; sample ST 75. Parallel light.
7–8). *Reticulofenestra rotaria* Theodoridis, ×2000; sample ST 75. (7) Parallel light; (8) crossed nicols.
9). *Helicosphaera sellii* Bukry and Bramlette, ×2000; sample ST 75. Parallel light.
10). *Discoaster pansus* (Bukry and Percival), ×1600; sample Gr 397. Parallel light.
11a). *Scyphosphaera apsteinii* Lohmann, b) *Scyphosphaera cantharellus* Kamptner, ×1600; sample Gr 398. Parallel light.
12a). *Scyphosphaera queenslandensis* Rade, b) *Scyphosphaera pacifica* Rade, ×1600; sample Gr 405. Parallel light.
13). *Amaurolithus delicatus* Gartner and Bukry, ×2400; sample Gr 405. Parallel light.
14). *Ceratolithus acutus* Gartner and Bukry, ×2000; sample Gr 405. Parallel light.
15). *Ceratolithus acutus* Gartner and Bukry, ×2400; sample Gr 405. Parallel light.

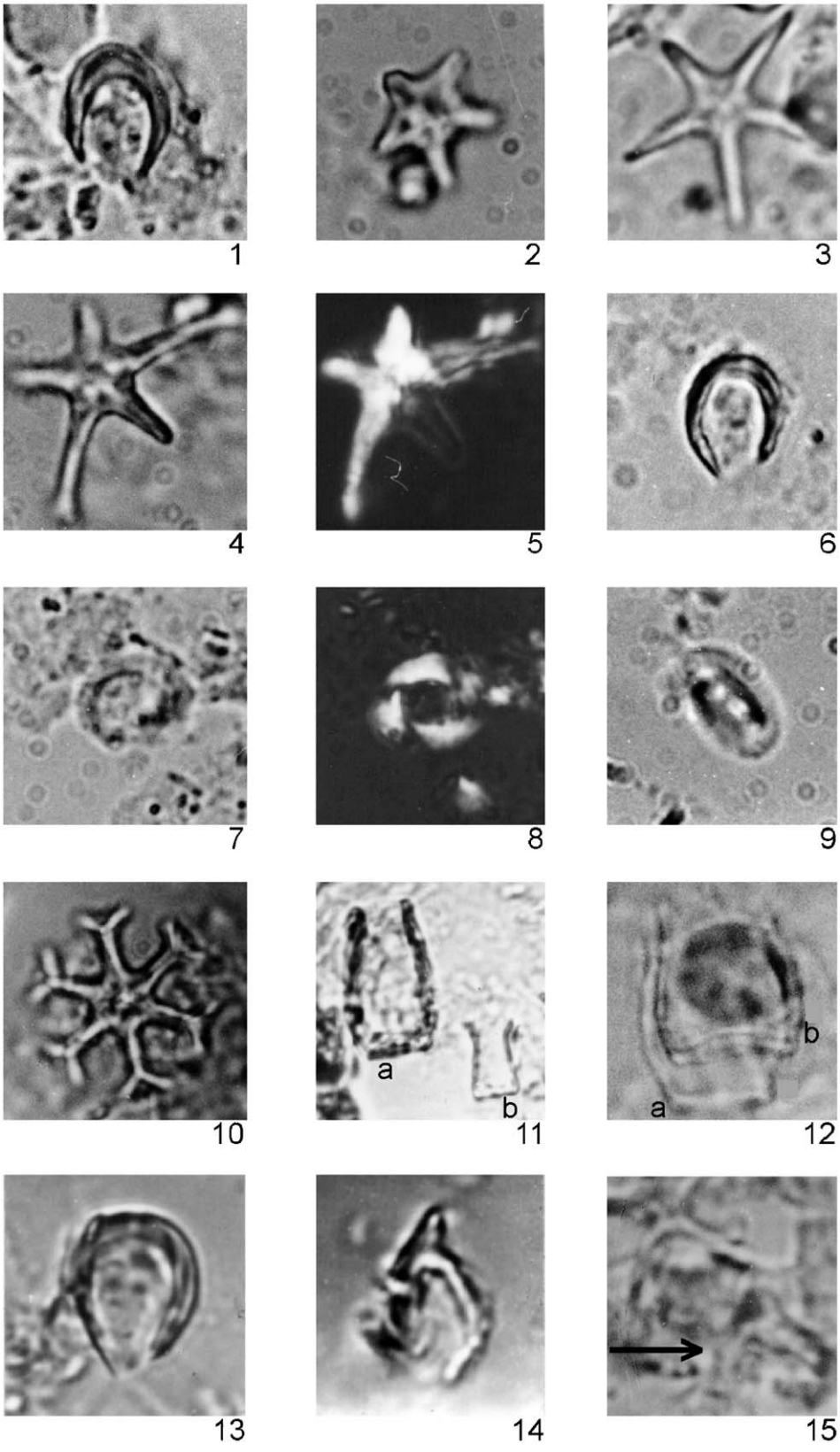
1
2
3
4
5
6
7
8
9
10
a
b
11
a
b
12
13
14
15

slightly better record with four polarity reversals was obtained from thin clay and silt beds between the coarse sands and gravels of section Labyrinthos. Two discontinuous intervals of normal polarity are interpreted: from 19 to 30 m and from 39 to 62 m, respectively, separated by an interval without samples and a level with reversed polarity at 38 m. The Dafni–Choumnikon transition, at 37.7 m after Gramann and Kockel (1969), corresponds to the end of an interval without samples, just below this reversed polarity level.

5. Calcareous nannofossils

5.1. Method

Samples were cut and rinsed to remove the weathered surface and to prevent contamination. Standard preparation techniques of Bramlette and Sullivan (1961) have been followed, supplemented by filtrating the samples with a 36 μm sieve. Smear slides were examined with a light microscope using transmitted and cross-polarized light at 1250× magnification.

5.2. Results

In most sections, with the positive exception of the relatively rich, upper parts of sections Kavala Road East and "Rema Marmara", occurrences of calcareous nannofossil assemblages are confined to thin intervals, separated by barren beds (Fig. 3). The results obtained from those samples that yielded assemblages with stratigraphic value are summarised below; a detailed compilation of our data is included in a distribution chart (Fig. 5). The indicated first and last occurrences should be interpreted with caution with respect to their biochronological meaning, given the generally irregular distribution of nannofossils and the partly low-resolution sampling in the sections of the Orphanic Gulf and Strimon Basin area. Zonal assignments are based on the Mediterranean MNN zonal scheme (after Raffi and Rio, 1979), a regionally valid modification of the NN-zonation of Martini (1971), and benefit from biostratigraphic observations and updates by Theodoridis (1984), Rio et al. (1990), Raffi et al. (2003) and Lourens et al. (2004).

5.2.1. Kavala Road West

The lowermost nannofossil assemblage, with *Helicosphaera stalis*, has been recovered from samples ST 67 and 68 (Figs. 3a and 5A). The co-occurrence of *Amaurolithus delicatus*, *A. primus*, *Discoaster misconceptus*, *D. quinqueramus*, *Reticulofenestra rotaria* and *Triquetrorhabdulus rugosus* in samples ST 73 and 74 (Plate I, 1–5) is considered, in accordance with Theodoridis (1984), to be indicative of Zone NN11b (the upper part of the *Discoaster quinqueramus*-Zone), i.e. Zone MNN11b–c. It is therefore plausible that the assemblage from the underlying samples ST 67 and 68 also belongs to Zone MNN11, possibly to its lower part.

In addition to the assemblage of samples ST 73 and 74, other species appear in the next-higher set of samples (ST 75 and Gr 395–399; Plate I, 6–11), such as *Amaurolithus bizzarus*, *Discoaster pansus*, *Helicosphaera sellii* and *Scyphosphaera* spp. *D. quinqueramus* was not identified. The co-occurrence in samples Gr 396, 398 and 405 (Plate I, 12–15) of — very rare — individuals of *Amaurolithus tricorniculatus*, *Ceratolithus acutus*, *C. larrymayeri* and *T. rugosus* characterizes the beginning of the Pliocene (sensu Theodoridis, 1984; Castradori, 1998; Van Couvering et al., 2000; Cavalezzi et al., 2002) and marks Zone MNN12. In the open ocean, the last occurrence of *D. quinqueramus* defines the end of Zone NN11. Using its

Plate II. Calcareous nannofossils from section "Rema Marmara", Orphanic Gulf area

1). *Discoaster pansus* (Bukry and Percival), ×3600; sample ST 37. Parallel light.
2). *Discoaster berggrenii* Bukry, ×4100; sample ST 40. Parallel light.
3). *Discoaster quinqueramus* Gartner, ×2900; sample ST 39. Parallel light.
4). *Discoaster quinqueramus* Gartner, ×3300; sample ST 44. Parallel light.
5). *Discoaster berggrenii* Bukry, ×4200; sample ST 47. Parallel light.
6). *Discoaster berggrenii* Bukry, ×4200; sample ST 47. Parallel light.
7–8). *Helicosphaera sellii* Bukry and Bramlette, ×2300; sample ST 50. (7) Parallel light; (8) crossed nicols.
9). *Discoaster giganteus* Theodoridis, ×1900; sample ST 51. Parallel light.
10–11). *Helicosphaera stalis* Theodoridis, ×3300; sample ST 50. (10) Parallel light; (11) crossed nicols.
12). *Triquetrorhabdulus rugosus* Bramlette and Wilcoxon, ×2400; sample Gr 1583. Parallel light.
13). *Amaurolithus delicatus* Gartner and Bukry, ×1800; sample ST 49. Parallel light.
14). *Amaurolithus primus* (Bukry and Percival), ×2200; sample ST 51. Parallel light.
15). *Triquetrorhabdulus rugosus* Bramlette and Wilcoxon, ×1700; sample ST 51. Parallel light.

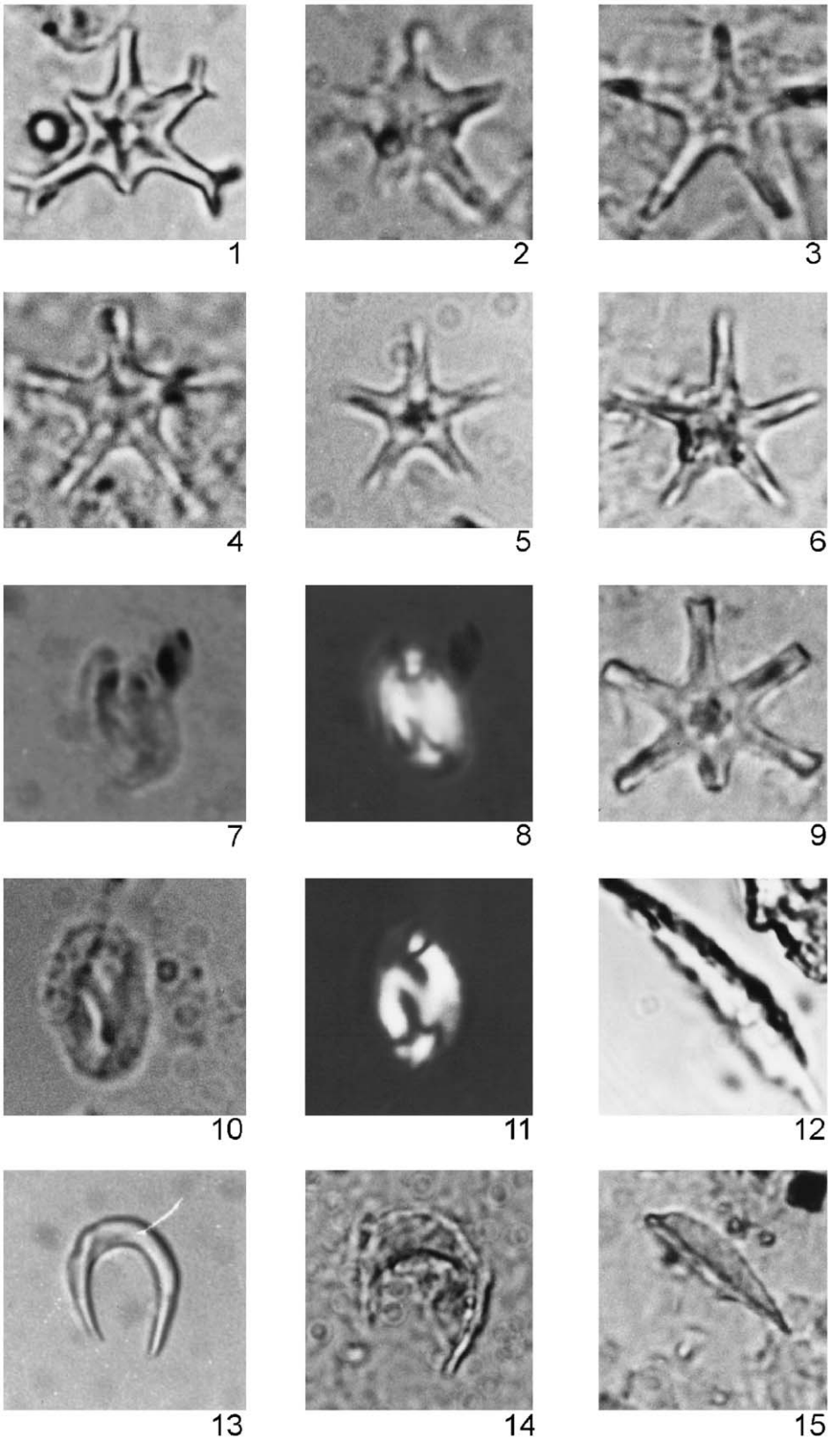
1
2
3
4
5
6
7
8
9
10
11
12
13
14
15

disappearance between samples ST 74 and ST 75 to identify here the debut of the *A. tricorniculatus*-NN12, or MNN12 Zone is debatable, given the generally rare occurrence (or absence) of *D. quinqueramus* in the Mediterranean toward the end of its range. The nannofossil assemblage of sample ST 75 is nevertheless interpreted to belong to Zone MNN12, because of its intermediate character when compared with the assemblages of the directly underlying (MNN11) and overlying Lower Pliocene (i.e. MNN12, upper part) samples. The last occurrences of *H. stalis* and *R. rotaria*, which species are not reported from levels higher than Zone MNN11b or -c (Negri and Villa, 2000; Raffi et al., 2003), may therefore be explained by reworking. The presence of *Helicosphaera* (cf. *H.*) *sellii*, first appearing in the Mediterranean in Zone MNN11 and absent in MNN12 until its re-entry in MNN13 (Rio et al., 1990), poses a similar problem. Possibly, the specimens found here, and in the following sections, are Miocene forms. *T. rugosus*, present up to sample Gr 397, disappears shortly after the first occurrences of *A. tricorniculatus* and *C. acutus*, exactly as in the Atlantic Ocean (Castradori, 1998; Raffi et al., 1998).

Samples Gr 400–422 contain a less diversified nannofossil assemblage, equally assignable to Zone MNN12. The assemblage of samples Gr 423, 424 and 428 consists, among others, of *A. delicatus* and *Ceratolithus rugosus*. The presence of *C. rugosus*, the nominate species of the *C. rugosus*-NN13, or MNN13 Zone, indicates a Zanclean age. No nannofossils were found in the top part of the section (samples Gr 413–419, 425–427, 429 and 430).

5.2.2. Kavala Road East

Sample ST 59 (Figs. 3A and 5A; Plate III, 1) yielded a very poor nannofossil assemblage, containing *Amaurolithus* sp., *H. stalis* and *T. rugosus*. The presence of *Amaurolithus* together with *H. stalis* suggests that this assemblage belongs to Zone MNN11b, in accordance with Negri and Villa (2000).

5.2.3. "Rema Marmara"

The assemblage identified in the top part of subsection I (sample ST 55; Figs. 3A and 5A) shows a low diversity, while samples ST 57 and 58 contain a more diversified assemblage with *H. stalis*. Calcareous nannofossils were recovered from a few sampling levels in the middle part of subsection II only. Sample ST 37 (Plate II, 1) contains numerous *Discoaster* species, such as *D. pansus* and *D. quinqueramus*, and can thus be assigned to Zone MNN11. The nannofossil content of the next-higher samples (ST 39 and 40; Plate II, 2–3) is dominated by *D. misconceptus*. Besides this species, *Discoaster berggrenii*, *R. rotaria* and *T. rugosus* are also present, together with rare specimens of *D. quinqueramus*. The assemblage of samples ST 55–58 is non-diagnostic, because it is composed of long ranging species that occur since the Middle Miocene. However, the micromammal fauna of the underlying beds was estimated to have a Middle Turolian age (De Bruijn, 1989), which implies that this level is correlative to the Upper Tortonian (Steininger et al., 1996). Consequently, the nannofossil assemblage of samples ST 55–58 may belong to Zone MNN11, also because in the overlying samples (ST 39–40) the co-occurrence of *D. quinqueramus* and *R. rotaria* indicates Zone MNN11b–c.

Sample ST 44, in subsection III, contains a relatively rich nannofossil assemblage with *D. quinqueramus* (Plate II, 4) and *H. stalis*. In the uppermost part of subsection III (samples ST 46–48; Plate II, 5–6) an assemblage with a large species variety is present, consisting, among others, of *D. berggrenii*, *Helicosphaera* (cf. *H.*) *sellii* and *R. rotaria*. These species co-occur with those identified

Plate III. Calcareous nannofossils from the Orphanic Gulf and Strimon Basin areas

1). *Amaurolithus* sp., ×1900; sample ST 59, section Kavala Road East. Parallel light.
2). *Amaurolithus delicatus* Gartner and Bukry, ×2800; sample Gr 440, section Akropotamos. Parallel light.
3). *Amaurolithus primus* (Bukry and Percival), ×2400; sample Gr 440, section Akropotamos. Parallel light.
4–5). *Helicosphaera sellii* Bukry and Bramlette, ×2800; sample ST 10, section Akropotamos. (4) Parallel light; (5) crossed nicols.
6). *Discoaster berggrenii* Bukry, ×2800; sample Gr 440, section Akropotamos. Parallel light.
7–8). *Scyphosphaera pacifica* Rade, ×1500; sample ST 8, section Akropotamos. (7) Parallel light; (8) crossed nicols.
9). *Amaurolithus* sp., ×3200; sample ST 120, section Ofrinion. Parallel light.
10). *Amaurolithus* cf. *A. primus* (Bukry and Percival), ×2100; sample ST 77, section Eziovis Rema. Parallel light.
11). *Amaurolithus primus* (Bukry and Percival), ×1800; sample ST 81, section Eziovis Rema. Parallel light.
12). *Braarudosphaera bigelowii* (Gran and Braarud), ×1200; sample ST 94, section Labyrinthos. Parallel light.
13). *Triquetrorhabdulus rugosus* Bramlette and Wilcoxon, ×1800; sample ST 93, section Labyrinthos. Parallel light.
14). *Amaurolithus primus* (Bukry and Percival), ×1800; sample ST 103, section Labyrinthos. Parallel light.
15). *Amaurolithus* sp., ×2000; sample ST 103, section Labyrinthos. Parallel light.

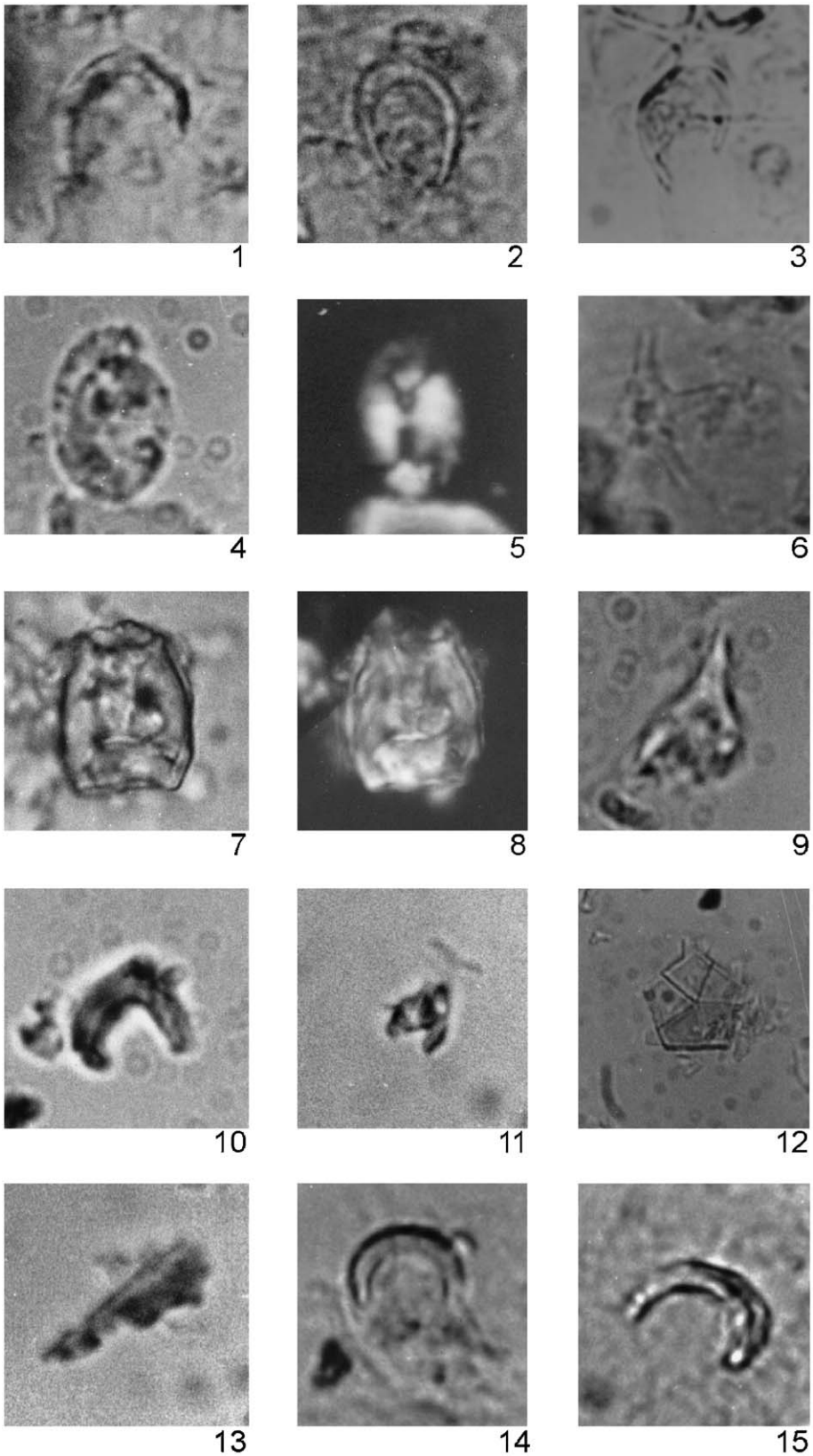
1
2
3
4
5
6
7
8
9
10
11
12
13
14
15

in sample ST 44. The presence of *D. quinqueramus*, *H. stalis* and *R. rotaria* suggests that the assemblages from this part of subsection III belong also to Zone MNN11b–c.

The nannofossil assemblage identified in samples ST 49–51 and Gr 1583 and 1584 from the upper part of subsection III shows high species abundances and diversities (Plate II, 7–15). Among the observed species are: *A. delicatus*, *A. primus*, *D. pansus*, *H. sellii*, *H. stalis*, *R. rotaria*, *Scyphosphaera* spp. and *T. rugosus*. The composition of this nannofossil assemblage is very similar to that in sample ST 75 of section Kavala Road West, which suggests that this assemblage belongs to Zone MNN12. This assignment is supported by the abundance ("acme") of *Scyphosphaera* found in these samples (see also Castradori, 1998; Siesser, 1998).

Reticulofenestra doronicoides is present in samples ST 55–58 and 46–51 in upwards increasingly high numbers, which is also occurring in Kavala Road West in samples ST 67–75. Similar observations were made in the Upper Miocene (Pontian) deposits from the western Black Sea margin (M. Mărunțeanu, unpublished data).

Sample ST 53, finally, contains a poor assemblage with *Sphenolithus abies* that can be assigned to Zones MNN12–MNN16 and thus probably being of Zanclean age.

5.2.4. Akropotamos

Re-examination of sample Gr 440 from subsection I (Figs. 3bBand 5B; Plate III, 2–3, 6) revealed that its nannofossil content, characterized by the co-occurrence of *A. delicatus*, *A. primus*, *D. berggrenii*, *D. misconceptus*, *Triquetrorhabdulus martini* and *T. rugosus*, belongs to Zone MNN11b–c, thus confirming the earlier assignment by Steffens et al. (1979).

In subsection II, only samples ST 6–10 from the upper part of the evaporite unit contain a rich nannofossil assemblage. It contains *A. delicatus*, *A. primus*, *D. berggrenii*, *D. misconceptus*, *Helicosphaera* (cf. *H.*) *sellii*, *H. stalis*, *T. rugosus* and various species belonging to the genus *Scyphosphaera* (Plate III, 4–5, 7–8). This assemblage is fairly similar to those identified higher in the Kavala Road West and "Rema Marmara" profiles. They differ by the presence of *D. quinqueramus* and *R. rotaria* and by the absence of *Lithostromation perdurum* and *Scyphosphaera* in the MNN11-assemblages of the latter sections. Although *D. quinqueramus* is absent in samples ST 6–10, the presence of *Amaurolithus* and *D. berggrenii* indicates that the nannofossil assemblage belongs to Zone MNN11b–c.

A far less diverse assemblage was observed in sample ST 25 of subsection III. The nannofossil assemblage recovered from the beds overlying this subsection, i.e. from the samples taken by Steffens et al. (1979): Gr 431–433, contains *Helicosphaera* cf. *H. sellii* (small and distorted specimens), together with very rare individuals of *A. delicatus* and *A. primus*. Samples Gr 434–438 contain a more diverse flora with, among others, common *Scyphosphaera* specimens, as well as rare specimens of *A. delicatus*, *A. primus* and (in sample Gr 436) *C. acutus*. The presence of the latter taxon indicates that the nannofossil assemblage is of Zanclean age and belongs to Zone MNN12.

5.2.5. Ofrinion

The laminated beds above the gypsum/anhydrite level (sample ST 120; Figs. 3B and 5B; Plate III, 9) contain a poor nannofossil assemblage, with very rare specimens of *A. bizzarus*, *Amaurolithus* sp. and *T. rugosus*. The occurrence of *Amaurolithus* suggests that this assemblage belongs to Zone MNN11b–c.

5.2.6. Eziovis Rema

The silts at the base of the calcareous beds contain a poor and badly preserved nannofossil assemblage (sample ST 77; Figs. 3B and 5B; Plate III, 10), with rare specimens of *A.* cf. *A. primus*, *Amaurolithus* sp. and *T. rugosus*. A similar assemblage, with rare *Amaurolithus primus*, was observed in sample ST 81 (Plate III, 11), taken from the separate outcrop on the southern side of the valley. Both assemblages with *Amaurolithus* belong, probably, to Zone MNN11b–c. It should be mentioned that the observed specimens of *Amaurolithus* are very small in size, in which respect they are fairly similar to those described by Mărunțeanu and Papaianopol (1998) and Snel et al. (2006-this volume) from Miocene–Pliocene transitional strata in Romania.

5.2.7. Labyrinthos

In the uppermost part of the Dafni Formation (samples ST 93 and 94; Figs. 4 and 5B; Plate III, 12–13), a nannofossil assemblage dominated by the presence of *Braarudosphaera bigelowii* was identified. Together with this species, small-sized and "regular-sized" *A. delicatus* and few individuals of *T. rugosus* were encountered. The presence of these species suggests that the assemblage belongs to Zone MNN11b–c or MNN12. Sample ST 94 has been taken from a clay cobble within the mass-flow bed, probably representing a reworked older level of the Dafni Formation.

The nannofossil assemblage of the Choumnikon Formation (samples ST 102 and 103; Plate III, 14–15) is, among others, composed of *Amaurolithus* cf. *A. primus*, *Amaurolithus* sp., *Scyphosphaera* sp. and *T. rugosus*. This assemblage may belong to Zone MNN11 b–c or MNN12 too. Other assemblages where *Amaurolithus* and low numbers of *Scyphosphaera* co-occur are found in samples ST 6–10 (Akropotamos), which are assigned to Zone MNN11b–c. In the profiles of Kavala Road West and "Rema Marmara", however, *Amaurolithus* and "peak" abundances of *Scyphosphaera* are confined to assemblages indicating Zone MNN12 (Fig. 5). We therefore suggest that the nannofossil levels from section Labyrinthos should be interpreted to belong to Zone MNN11b or -c.

6. Palaeobathymetry

An estimate of the depositional depth was made for the upper parts of sections Kavala Road West (samples ST 75 and Gr 395–428), "Rema Marmara" (ST 44–53 and Gr 1583–1585) and Akropotamos (Gr 431–438). This estimate is based on the general relation between depth and the fraction of planktonic planktonic foraminifera with respect to the total foraminiferal population of Van der Zwaan et al. (1990), following procedures of Van Hinsbergen et al. (2005). Additionally, an independent check of the calculated depth was carried out, using the depth chart of selected species of benthic foraminifera of Van Hinsbergen et al. (2005).

The results are listed in Fig. 6. Most samples contain high amounts of quartz and rock fragments, which are indicative of down-slope (mass) transport. Therefore, the calculated depth should be considered as minimum depth values. Moreover, since the foraminifera-bearing intervals of the three sections contain alternating homogeneous silts and sapropelitic layers, clear evidence exists for fluctuating oxygen levels of the bottom waters during sediment deposition. Since the oxygen level has a profound effect on the intensity of benthic life, the calculated depth values should be regarded as rough estimates. The independent check using the benthic foraminiferal depth markers forms a more reliable depth measure. As a rule, the deepest markers indicate the depositional depth.

section	n	depth		
		calculated		taxonomic
		depth	SD	estimate
Kavala Road West	16	368	194	500-900
"Rema Marmara"	3	398	258	300-600
Akropotamos	4	518	236	500-900

Fig. 6. Palaeobathymetry estimates for the sections of Kavala Road West, "Rema Marmara" and Akropotamos. '*N*' is the number of analysed samples. An independent check of the depositional depth for a selection of the samples, using the depth chart of selected species of benthic foraminifera (Van Hinsbergen et al., 2005), is given in the right hand column.

The benthic foraminiferal content of samples ST 75, Gr 412 and 428 (of the Kavala Road West section), of sample Gr 1585 ("Rema Marmara") and of sample Gr 431 (Akropotamos) was analysed. The samples of section Kavala Road West contain a diverse and rich deep-marine fauna, including *Karreriella bradyi*, *Cibicides robertsonianus*, *C. bradyi*, *C. kullenbergi*, *Oridorsalis* spp., *Planulina ariminensis* and *Siphonina reticulata*, indicating a depositional depth of at least 500 m. The absence of *Cibicides italicus* and *C. wuellerstorfi* indicate a maximum depth of approximately 900–1000 m. Sample Gr 1585 of section "Rema Marmara" contains *Oridorsalis* spp., *P. ariminensis*, *Uvigerina* spp., *Cibicides pachydermus* and *C. pseudoungerianus*, indicative of a depth of 300–600 m. Sample Gr 431 of section Akropotamos contains *K. bradyi*, *Cibicoides kullenbergi*, *S. reticulata* and *P. ariminensis*, which indicate a bathymetry comparable to the one obtained for the Kavala Road West section: 500–900 m (Fig. 6).

A large discrepancy exists between the calculated depth and the depth estimate obtained by the analysis of depth markers. Although evidence for down-slope transport is given by the high amounts of quartz and rock fragments, shallow water markers such as *Ammonia beccarii*, *Cibicides lobatulus*, *Elphidium* spp. and *Discorbis* spp. are generally absent or present in low quantities. Possibly, relative enrichment of benthic foraminifera occurred as a result of winnowing, removing the lighter plankton fraction. If this was the case, the water column directly overlying the sediment-water interface must have been in motion throughout the deposition of the Pliocene of the Strimon basin, possibly in a submarine canyon system.

7. Stratigraphic framework and regional correlations

In this section, we attempt to establish an integrated stratigraphic framework for the Orphanic Gulf area and the Strimon Basin. At first, this will be done separately for the two areas through the combination of nannofossil biostratigraphy, (lithostratigraphic) correlation of marker

beds and the incorporation of paleomagnetic data. The two frameworks will then be correlated with the Mediterranean and (Eastern) Paratethys stages, respectively. This, in turn, will facilitate exploring the interaction between the Mediterranean and the Paratethys in Late Miocene to Early Pliocene time.

7.1. Orphanic Gulf area

Our nannofossil results show that the marine and brackish successions of the five sections exposed along the Orphanic Gulf (Fig. 1) cover the greater part of Zones MNN11, MNN12 and MNN13 (Figs. 3 and 5). Consequently, these sections jointly comprise (part of) the Upper Miocene and the Lower Pliocene. A number of key beds can be used to refine the correlation between the Orphanic Gulf sections (Fig. 7).

The first and most prominent correlation level is the travertine marker bed overlying sandstone or gravel units in sections Kavala Road West, Kavala Road East, "Rema Marmara" and Akropotamos (line 'T'; Fig. 7). This relatively thick limestone bed represents a clear geomorphological feature. Below it, 10–20 m of fine-grained, often laminated brackish water sediments can be observed (not exposed in "Rema Marmara"), which, in turn, covers a gypsiferous interval of approximately 10 m in sections Kavala Road East and Akropotamos. A comparable succession of evaporites and overlying laminites is also exposed in the top of the Ofrinion profile (Fig. 3b). The nannofossil assemblages of samples ST 6–10 (Akropotamos: at 10 m in subsection II; Fig. 3b) and ST 120 (Ofrinion: at 59 m; Fig. 3b), although being quite different in species (Fig. 5b) and numbers of specimens, both were recovered from levels within the evaporite unit and both probably belong to Zone MNN11b or -c. Therefore, these evaporites and nannofossil assemblages are tentatively related to the same marine phase. The gypsum beds in section Akropotamos were proposed to correspond to the Messinian evaporites found elsewhere in the Mediterranean (Meulenkamp, 1979; Dermitzakis et al., 1986). These and the other gypsiferous beds of the Orphanic Gulf area may form the, presently onshore, equivalent of the evaporites of the Nestos–Prinos–Kavala Basin near the island of Thasos, where they are up to 800 m thick and include halite cycles (Pollak, 1979; Proedrou, 1979). Indeed, the presence of nannofossil assemblages containing *Amaurolithus* spp. (with a first occurrence at 7.42 Ma: Raffi et al., 2003) below and above the Orphanic Gulf area evaporites gives a possible Messinian age range for these evaporites, which is consistent with that of the Lower or Upper Evaporites in the Mediterranean (5.96–5.59 or 5.50–5.33 Ma: Krijgsman et al., 1999). The base of the gypsum/anhydrite beds of sections Akropotamos, Kavala Road East and Ofrinion (line 'E'; Fig. 7) is tentatively correlated with the base of the Lower Evaporites.

Evaporites are absent in sections Kavala Road West and "Rema Marmara" (Fig. 3a). There, shallow marine calcareous and sandy beds with *Ditrupa* (in Kavala Road West between 95 and 100 m; in "Rema Marmara" at 40 m in subsection I) constitute an alternative correlation level. Nannofossil assemblages of samples ST 55–58 ("Rema Marmara") and samples ST 67 and 68 (Kavala Road West), found close to the *Ditrupa* levels, are correlated with sample ST 59 below the evaporites of Kavala Road East (at 42 m; Fig. 3a). The base of the interval of laminated clays, silts and platy limestones above the calcareous *Ditrupa* beds and below the travertine unit, i.e. at 102 m in Kavala Road West, is suggested to be correlative to the base of the evaporites (Fig. 7). This suggestion is supported by the lithological resemblance of the thin-bedded shallow marine beds directly above the gypsum, in sections Akropotamos (between 13 and 28 m in subsection II) and Ofrinion (from 58 m onward; Fig. 3b), and the similarly laminated, brackish beds between 102 and 120 m in Kavala Road West. In "Rema Marmara", the interval between the *Ditrupa* and travertine levels of subsections I (top) and II (base), respectively, is unexposed.

The very similar post-travertine beds of sections Kavala Road West and "Rema Marmara" allow a good general litho- and biostratigraphic correlation. Their nannofossil assemblages show diversification in Zones MNN11b–c to MNN12, associated with a rapid change from brackish clays and silts to open marine marls and sapropels (Fig. 3a). Sands and conglomerates are found at the top of both sections. In detail, however, some differences are evident. The main lithological distinction between the sediments exposed between the travertine marker bed and the Pliocene sapropelitic beds in Kavala Road West and "Rema Marmara" is the presence of an intercalation of coarse clastics in the latter section (Figs. 3a and 7). This difference is attributed to the more proximal position of "Rema Marmara" relative to the basin margin.

According to the nannofossil record (Fig. 5a), the short interval at 153 m in section Kavala Road West, between samples Gr 395 and 396 (where an assemblage with *C. acutus* appears: correlation line labelled '3'; Fig. 7), should correspond to the Miocene–Pliocene transition. A still younger assemblage, belonging to Zone NN13, is present below the conglomerates at the top of

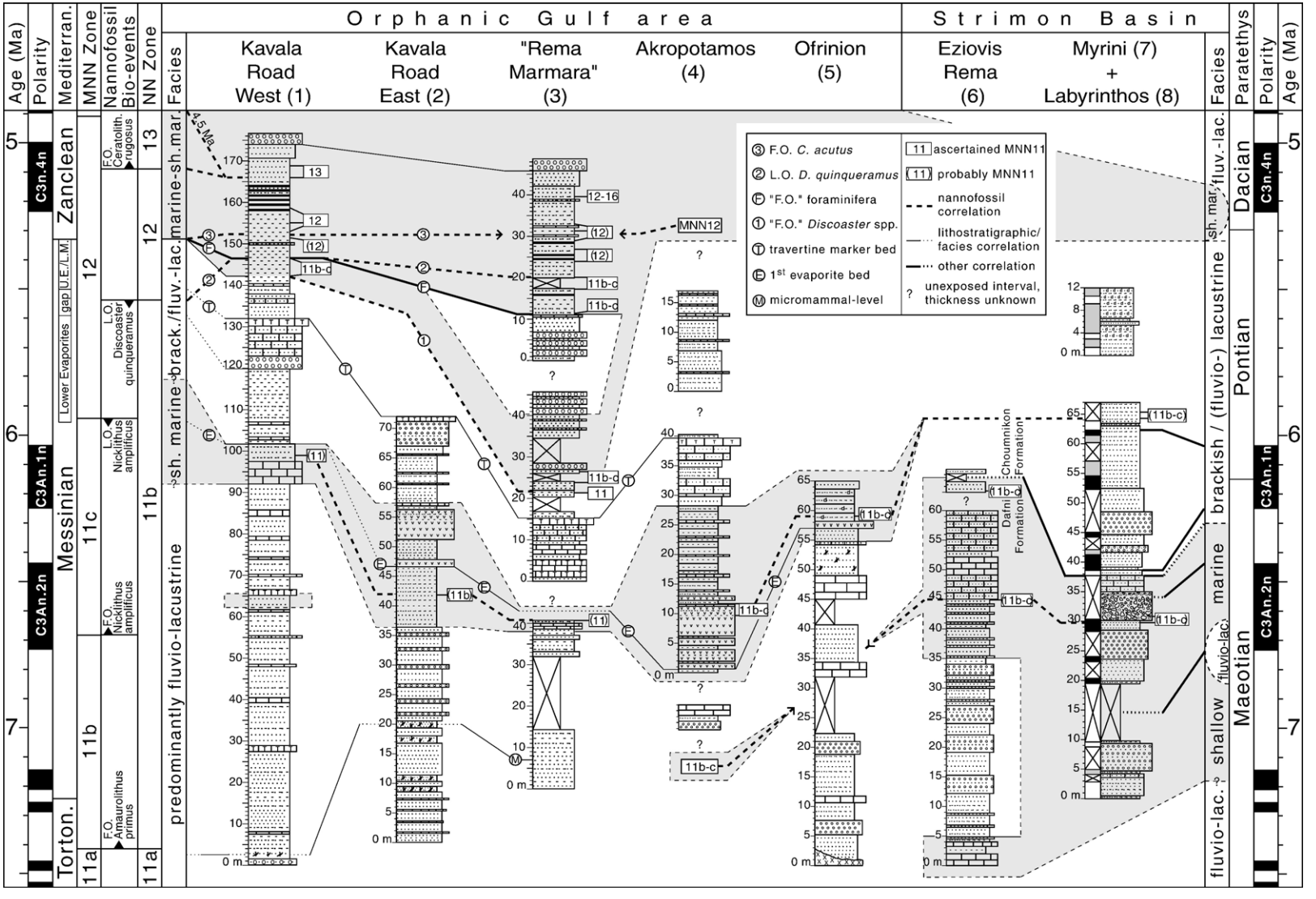

Fig. 7. Correlation of Upper Miocene to Lower Pliocene sections of the Orphanic Gulf and Strimon Basin areas (numbered as in Fig. 1) with calcareous nannofossil zones and bio-events (after Martini, 1971; Raffi and Rio, 1979; Raffi et al., 2003), with the Astronomical Tuned Neogene Time Scale (after Lourens et al., 2004) and with the Eastern Paratethys (Dacic Basin) age calibration (after Snel et al., 2006-this volume). The correlation lines labelled '1', 'F', '2' and '3' refer to local observations of first and last occurrences of calcareous nannofossil species and of benthic and planktonic foraminiferal taxa in sections Kavala Road West and "Rema Marmara". Intervals with a presumed marine depositional environment are shaded. Facies of the Messinian salinity crisis are after Krijgsman et al. (1999); U.E./L.M. denotes Upper Evaporites/Lago Mare.

this section. Conversely, in the open marine part of subsection III in "Rema Marmara" Pliocene marker species of the family Ceratolithaceae were not found. Hence, the nannofossils cannot be used to identify the Miocene–Pliocene boundary here.

An alternative indication for this boundary, and more consistent with the facies change both in sections Kavala Road West and "Rema Marmara", is the appearance of rich and diversified benthic and planktonic foraminiferal associations. In Kavala Road West and "Rema Marmara" these foraminiferal faunas, which might reflect the local impact of the earliest Pliocene flooding, are found upwards from sampling levels ST 74 and ST 44, respectively (Figs. 3a and 7; correlation line 'F'). Unfortunately, the foraminiferal associations lack any Pliocene index taxa, which prevents drawing sound conclusions on the discrepancy between calcareous nannofossils and foraminifera with respect to the position of the Miocene–Pliocene transition in this area. Likely, this discrepancy is caused by environmental control on the appearance level of the Pliocene nannofossil markers. The *Amaurolithus* and *Ceratolithus* species are relatively rare and easy to miss, particularly in the sediments from the studied area. The presence of MNN11 — *Discoaster* — marker species in the open marine marl interval, found even above the first sapropel up to 21 m in subsection III in "Rema Marmara" (Fig. 3a), can be explained by reworking.

The fossil soils and red beds of the basal part of the sections along Kavala Road, and possibly the palaeo-sol below the gypsiferous bed of section Ofrinion, are the youngest continental deposits and might be correlative to the upper Tortonian level with Zone MN12 micromammal fossils at the base of section "Rema Marmara" (labelled 'M'; Fig. 7).

7.2. Strimon Basin

The nannofossil assemblages recovered from the Dafni and Choumnikon beds of sections Eziovis Rema and Labyrinthos (Figs. 3b and 4) may, as we suggested before, belong to Zone MNN11b–c. The correlation of the Dafni and Choumnikon Formations with the (Paratethys) Maeotian and Pontian stages, respectively (Gramann and Kockel, 1969; Popov and Nevesskaya, 2000), and the recently established magnetostratigraphy of the Maeotian and Pontian sediments in Romania (Snel et al., 2006-this volume) are in agreement with this presumption (Fig. 7). The position of samples ST 102 and 103 in Labyrinthos (at 65 m; Fig. 4) in an interval with reversed magnetic polarity, above a normal polarity interval of the (Pontian) Choumnikon beds, suggests an age estimate for these levels with nannofossil assemblages younger than 6.04 Ma: the age of the end of subchron C3An.1n (Krijgsman et al., 1999). The age of sample ST 93, located at 30 m in the lower normal polarity interval of the upper part of the (Maeotian) Dafni beds, which we assume to represent subchron C3An.2n, can be estimated at approximately 6.5 Ma. A similar age can be assigned to sample ST 77 of section Eziovis Rema (45 m; Fig. 3b), taking into account its position relative to the position of the Dafni–Choumnikon transition.

Considering the above, the reversed-to-normal polarity reversal between 38 and 39 m in section Labyrinthos is interpreted to represent the base of normal subchron C3An.1n, dated at 6.26 Ma by Krijgsman et al. (1999). The age of the Dafni-Choumnikon boundary is thus estimated at approximately 6.3 Ma, which is slightly older than the age estimate of the Maeotian–Pontian transition in the Dacic and Euxinic basins (6.15 Ma: Snel et al., 2006-this volume). Popov and Nevesskaya (2000) noted, however, that the lowermost part of the Choumnikon Formation in Labyrinthos contains mollusc species deviating from the typical Pontian assemblages. True Pontian-type molluscs are found from approximately 50 m onward, a level corresponding to the middle of C3An.1n, which is more closely resembling the Eastern Paratethys' position of the base of the Pontian.

The Choumnikon beds in the section of Myrini, with exclusively reversed polarity, are likely younger than the highest beds we recorded at the section of Labyrinthos (Fig. 4). The oyster beds found directly above the Myrini quarry probably correspond to the same shallow marine phase as the Pliocene oyster-bearing clays sampled at Labyrinthos by Popov and Nevesskaya (2000).

7.3. Correlation of the Orphanic Gulf and Strimon Basin sequences

Our biostratigraphic and chronostratigraphic data demonstrate that the fluvio-lacustrine and shallow marine to brackish Messinian sequences of the Orphanic Gulf area are correlative with the shallow marine and brackish beds of the Dafni and Choumnikon Formations of the Strimon Basin (Fig. 7). This correlation depends on the estimated age of the Maeotian–Pontian boundary (Snel et al., 2006-this volume), which has been suggested to be coeval with the Dafni–Choumnikon boundary (Gramann and Kockel, 1969; Popov and Nevesskaya, 2000), and on the assumption that the Orphanic Gulf evaporites are coeval with the evaporites

of the Messinian salinity crisis (Meulenkamp, 1979; Dermitzakis et al., 1986).

In view of the above, it would be reasonable to correlate the nannofossil assemblages obtained from or close to the evaporites (samples ST 6–10 of section Akropotamos, at 10 m in subsection II, and sample ST 120 of section Ofrinion, at 59 m; Fig. 3b) with those of samples ST 102 and 103 of the Choumnikon beds of section Labyrinthos (at 65 m; Fig. 4), since these latter samples probably have a comparable — Late Messinian — age. The observation that their nannofossil assemblages are in fact similar, although less diverse (Fig. 5b), to those of samples ST 6–10, does not contradict this correlation. The lowest level with nannofossils in the Akropotamos section is tentatively correlated with the oldest assemblages in the Dafni beds of the Strimon area, which would give this level an approximate age of 6.5 Ma (Fig. 7). The first shallow marine sediments in the Kavala Road West section (the oyster bed at 65 m; Fig. 3a) could have a comparable age. Subsequently, above the evaporites, the lacustrine travertinous interval of the Orphanic Gulf area may correspond to the lacustrine diatomaceous clays and silts exposed in the Myrini quarry. The overlying shallow marine deposits, found on top of both this last section and Labyrinthos, are straightforwardly linked with the Pliocene marine strata exposed along the Orphanic Gulf.

Although the comparisons between the nannofossil assemblages of the Orphanic Gulf and Strimon basin areas should not be regarded as detailed, bed-to-bed correlations, alternative solutions are, in our opinion, less probable. The assumption of synchronism of the marine evaporite and *Ditrupa* beds (lower grey-shaded belt in Fig. 7) of the Orphanic Gulf area sections with the marine Dafni beds of the Strimon Basin, implicates that either these evaporites are older than the Messinian evaporites in the rest of the Mediterranean, or that the Dafni and Choumnikon Formations would have a much younger age. Besides, this last option would exclude the direct correlation of these formations with the Maeotian and Pontian and be in conflict with our interpretation of the paleomagnetic results of section Labyrinthos.

8. Discussion and conclusions

The Neogene deposits allow to explore the general palaeogeography of the Orphanic Gulf–Strimon Basin area and to reconstruct the exchange of water masses between the Mediterranean and the Paratethys before, during and after the Messinian salinity crisis.

Upper Vallesian (MN11, in the Lefkon Formation) and Middle Turolian (MN12, in subsection I of "Rema Marmara") mammal faunas record the debut and the end of continental deposition in the Strimon Basin and Orphanic Gulf areas, respectively (De Bruijn, 1989). Subsequently, in the course of the latest Tortonian/Early Messinian, we find the onset of a shallow marine phase in the Strimon Basin, witnessed by the marine beds of the Dafni Formation (Figs. 2 and 7). The Orphanic Gulf area was at first flooded only locally, as can be observed in Kavala Road West and Akropotamos. More widespread, but still shallow marine conditions existed in this area in the beginning of the Late Messinian, during deposition of the Choumnikon Formation in the Strimon Basin. After the marine interval, a phase of brackish to freshwater conditions occurred in the Orphanic Gulf area too, lasting until the end of the Messinian. In the Early Pliocene, both areas were connected to the open sea again. In the Strimon Basin this ingression was very brief and only shallow marine sedimentation took place, whereas in the coastal area along the Orphanic Gulf deep marine successions were deposited. Finally, in the Plio-Pleistocene, basin infill by renewed massive supply of predominantly coarse clastics led to fluvio-deltaic conditions in the Orphanic Gulf and Strimon Basin areas as before in the Tortonian.

The mixed mollusc faunas from the Dafni and Choumnikon beds show that the Strimon Basin formed (part of) a transitional area between the Mediterranean and the Eastern Paratethys in Messinian/Maeotian–Pontian time (Gramann and Kockel, 1969; Popov and Nevesskaya, 2000). Atlantic–Mediterranean influence in the pre-Pontian Aegean successions during the Maeotian (first half of the Messinian) is illustrated by the presence of marine beds, frequently reefal limestones, including the Dafni beds of the Strimon Basin and the Trakones limestones near Athens (Gramann and Kockel, 1969; Stevanoviæ, 1990). Furthermore, marine mollusc faunas and nannofossils were recovered from Maeotian deposits in the Ponto-Caspian Basin (Gramann and Kockel, 1969; Semenenko and Pevzner, 1979; Mărunțeanu and Papaianopol, 1998; Nevesskaya et al., 2003), suggesting ingressions from the Atlantic–Mediterranean realm. Also during the Pontian time, we conclude that intermittent palaeogeographical connections with the Paratethys existed (supposedly via the Aegean area), as is indicated by the discontinuous distribution of levels with nannofossils intercalated in successions of Pontian/Late Messinian age in the Orphanic Gulf–Strimon Basin area and in the Dacic and Euxinic basins (Mărunțeanu and Papaianopol,

1998; Snel et al., 2006-this volume). Our conclusion on the ephemeral spilling of Atlantic Ocean waters into the Mediterranean Basin during the Pontian / Late Messinian is corroborated by the observations of Castradori (1998), who reported nannofossil assemblages (although anomalous, indicating unfavourable conditions) from the stratigraphic equivalent of the Lago Mare Formation, in ODP Site 967 in the Eastern Mediterranean and in Sites 975 and 978 in the Western Mediterranean.

Aside from these brief marine incursions from the Mediterranean, the opposite, i.e. invasion of brackish (Eastern) Paratethys waters in the Aegean domain, prevailed during the Pontian/Late Messinian. Brackish water faunas, typical for the Early Pontian, are present in the Orphanic Gulf–Strimon Basin area (from 6.3 Ma onward: the age of the base of the Choumnikon Formation) and are also found further to the east in the Xanthi–Komotini Basin, as well as near Athens in the Trakones area and on the island of Aegina (Papp and Steininger, 1979; Rögl et al., 1991; Syrides, 1998). In the Orphanic Gulf area, Paratethyan faunas were observed only after the interval of evaporite deposition (Steffens et al., 1979), as in the Lago Mare Formation throughout many parts of the Mediterranean.

The Messinian salinity crisis is characterized by a widely recognised erosional surface across the Mediterranean, including canyons in the margins (Chumakov, 1973; Clauzon, 1973; Hsü et al., 1973; Cita and Ryan, 1978). The responsible regional sea-level drop is also recorded in sequences of the Black Sea Basin, in the uppermost part of the Miocene, and has been discussed by Hsü (1978), Hsü and Giovanoli (1979), Kojumdgieva (1983) and, more recently, by Clauzon et al. (2005) and Popescu (2006-this volume). The erosional surface on the Black Sea margin (Hsü and Giovanoli, 1979) and a pre-Pliocene unconformity at the entrance of the Danube in the western part of the Dacic Basin (Clauzon et al., 2005) were interpreted to express the effects of the climax of the Messinian salinity crisis on the Eastern Paratethys. The corresponding desiccation event must equally have affected the Orphanic Gulf–Strimon Basin area. Indeed, we suggest that the Late Messinian stage of isolation of the Mediterranean from the Atlantic Ocean resulted in deposition of the non-marine unit of gravel/sandstone and topping travertine marker bed (indicated by line 'T'; Fig. 7). The basin-wide effect of the desiccation event can explain that this laterally uniform, sedimentary unit covers a relatively large part of the Orphanic Gulf area.

However, we did not find evidence for a prolonged phase of erosion persisting until the Early Pliocene, as proposed by Clauzon et al. (1996) for the marginal basins of the Mediterranean Sea. Instead, the consistent sequence of evaporite–brackish water–travertine–brackish water beds in the sections of Kavala Road, "Rema Marmara" (even with nannofossil levels between the travertines and the Pliocene marls; Fig. 3a) and Akropotamos, which predates the open marine Pliocene beds (Fig. 7), suggests that after the (brief) erosional phase aquatic conditions were restored. The inferred marine ingressions in the deep Mediterranean basins (Castradori, 1998) and in the marginal basins of our Northern Aegean study area as well as in the Dacic Basin (Snel et al., 2006-this volume), before the beginning of the Pliocene, question a deep basin–shallow water scenario for the entire Late Messinian. Provided that the foraminifera beds of in the Orphanic Gulf area belong to the very base of the Zanclean, the period of desiccation thus occurred before the end of the Messinian (and Pontian) stage, and probably between the intervals of the Lower Evaporites and the Lago Mare of the Mediterranean Basin: in line with the 'gap' at 5.59–5.50 Ma of Krijgsman et al. (1999).

The Dafni–Choumnikon transition in the Strimon Basin, where the strata of both formations cover roughly the same area, appears to be characterized by a rapid environmental change from marine to brackish water conditions, without a changing basin configuration (Gramann and Kockel, 1969). Similarly, the Miocene–Pliocene boundary of the Orphanic Gulf area seems to comprise the transition from brackish environments to open marine conditions, possibly through improved connections of the Atlantic and Mediterranean areas. The sudden appearance of benthic and planktonic foraminifera suggests a rapid relative rise of sea level. Our palaeobathymetry data show that the Orphanic Gulf area was already a relatively deep basin in the Early Pliocene (500–900 m; Fig. 6). In this area, subsidence kept pace with sedimentation during the Late Tortonian/Early Messinian, until the deposition of shallow water evaporites. We suggest that between this moment and the Early Pliocene increased subsidence occurred. However, we found no indications for a tectonically induced transgression, caused by ongoing subsidence, at the beginning of the Pliocene. The presence of brackish water faunas and intercalated nannofossil assemblages in the highest part of the Messinian illustrates that, before the Early Pliocene, the basin was not completely desiccated. It might even be possible that in this part of the Northern Aegean no Pliocene flooding proper

occurred. Perhaps, the Miocene–Pliocene transition was merely marked here by a change of salinity, caused by the increasing influence of Atlantic–Mediterranean over Paratethyan waters.

Acknowledgements

Hans de Bruijn (Utrecht) and George Syrides (Thessaloniki) are gratefully thanked for their invaluable guidance, sampling efforts and discussions in the field. The efforts of Constantin Doukas (Athens), to arrange the necessary permits and to solve logistical problems, are highly appreciated. Stefan Garstman is thanked for his skilful assistance in paleomagnetic sampling. We also thank Geert Ittmann and Gerrit van 't Veld for providing washed/sieved samples and nanno-smear-slides, and Douwe van Hinsbergen for carrying out palaeo-bathymetry analyses. We particularly thank the reviewers Isabella Raffi and Sylvia Iaccarino for critically reviewing an earlier version of the manuscript, and also Davide Castradori, Frits Hilgen and Cor Langereis for their valuable comments.

This work was conducted under the programme of the Netherlands Research School of Sedimentary Geology (NSG). The Netherlands Research Centre for Integrated Solid Earth Science (ISES) provided funds for visiting research fellowships for the second author (M.M.) and for sampling campaigns. This is NSG publication 20021204.

References

Armour-Brown, A., Bruijn, H. de, Maniati, C., Siatos, G., Niesen, P., 1979. The geology of the Neogene sediments north of Serrai and the use of Rodent faunas for biostratigraphic control. Proceedings of the 6st Colloquium on the Geology of the Aegean Region, Athens 1977, 2, pp. 615–622.

Bornovas, J., Rondogianni-Tsiambaou, Th., 1983. Geological map of Greece, 2nd edition. Institute of Geology and Mineral Exploration, Athens.

Bramlette, M.N., Sullivan, F.R., 1961. Coccolithophorids and related nannoplankton of the Early Tertiary in California. Micropaleontology 7 (2), 129–188.

Castradori, D., 1998. Calcareous nannofossils in the basal Zanclean of the Eastern Mediterranean Sea: remarks on paleoceanography and sapropel formation. Proceedings of the Ocean Drilling Program. Scientific Results 160, 113–123.

Cavalezzi, B., Raffi, I., Biondi, R., 2002. Ceratoliths in the lowermost Pliocene of the Eastern Mediterranean: correlation to the equatorial Atlantic (poster). Journal of Nannoplankton Research 24 (2), 81.

Chumakov, I.S., 1973. Pliocene and Pleistocene deposits of the Nile Valley in Nubia and Upper Egypt. Initial Reports of the Deep Sea Drilling Project 13, 1242–1243.

Cita, M.B., Ryan, W.B.F., 1978. Messinian erosional surfaces in the Mediterranean. Marine Geology 27, 1–366.

Clauzon, G., 1973. The eustatic hypothesis and the pre-Pliocene cutting of the Rhone Valley. Initial Reports of the Deep Sea Drilling Project 13, 1251–1256.

Clauzon, G., Suc, J.-P., Gautier, F., Berger, A., Loutre, M.-F., 1996. Alternate interpretation of the Messinian salinity crisis: controversy resolved? Geology 24 (4), 363–366.

Clauzon, G., Suc, J.-P., Popescu, S.-M., Mărunţeanu, M., Rubino, J.-L., Marinescu, F., Melinte, M.C., 2005. Influence of Mediterranean sea-level changes on the Dacic Basin (Eastern Paratethys) during the late Neogene: the Mediterranean Lago Mare facies deciphered. Basin Research 17, 437–462.

De Bruijn, H., 1989. Smaller mammals from the Upper Miocene and Lower Pliocene of the Strimon basin, Greece: Part 1. Rodentia and Lagomorpha. Bollettino della Società Paleontologica Italiana 28 (2–3), 189–195.

Dermitzakis, M.D., Georgiades-Dikeoulia, E., Velitzelos, E., 1986. Ecostratigraphic observations on the Messinian deposits of Akropotamos area (Kaval, N. Greece). Annales Géologiques des Pays Helléniques 33, 367–376.

Dinter, D.A., 1998. Late Cenozoic extension of the Alpine collisional orogen, northeastern Greece: origin of the north Aegean basin. Geological Society of America Bulletin 110 (9), 1208–1230.

Dinter, D.A., Royden, L., 1993. Late Cenozoic extension in northeastern Greece: Strymon Valley detachment system and Rhodope metamorphic core complex. Geology 21, 45–48.

Gramann, F., Kockel, F., 1969. Das Neogen im Strimonbecken (Griechisch–Ostmazedonien). Teil 1: Lithologie, Stratigraphie und Paläogeographie. Geologisches Jahrbuch 87, 445–484.

Hsü, K.J., 1978. Stratigraphy of the lacustrine sedimentation in the Black Sea. Initial Reports of the Deep Sea Drilling Project 42B, 509–524.

Hsü, K.J., Giovanoli, F., 1979. Messinian event in the Black Sea. Palaeogeography, Palaeoclimatology, Palaeoecology 29, 75–93.

Hsü, K.J., Cita, M.B., Ryan, W.B.F., 1973. The origin of the Mediterranean evaporites. Initial Reports of the Deep Sea Drilling Project 42, 1203–1231.

Karistineos, N.K., Georgiades-Dikeoulia, E., 1986. The marine transgression in the Serres basin. Annales Géologiques des Pays Helléniques 33, 221–232.

Kojumdgieva, E., 1983. Palaeogeographic environment during the desiccation of the Black Sea. Palaeogeography, Palaeoclimatology, Palaeoecology 43, 195–204.

Krijgsman, W., Hilgen, F.J., Raffi, I., Sierro, F.J., Wilson, D.S., 1999. Chronology, causes and progression of the Messinian salinity crisis. Nature 400, 652–655.

Lourens, L.J., Hilgen, F.J., Laskar, J., Shackleton, N.J., Wilson, D., 2004. The Neogene period. In: Gradstein, F.M., Ogg, J.G., Smith, A.G. (Eds.), A Geologic Time Scale 2004. Cambridge University Press, Cambridge, pp. 409–440.

Martini, E., 1971. Standard Tertiary and Quaternary calcareous nannoplankton zonation, In: Farinacci, A. (Ed.), Proceedings of the 2nd International Conference on Planktonic Microfossils, Roma 1970, 2, ed. Tecnoscienza, Rome, pp. 739–785.

Mărunţeanu, M., Papaianopol, I., 1998. Mediterranean calcareous nannoplankton in the Dacic Basin. Romanian Journal of Stratigraphy 78, 115–121.

Meulenkamp, J.E., 1979. The Aegean and the Messinian salinity crisis. Proceedings of the 6st Colloquium on the Geology of the Aegean Region, Athens 1977, 3, pp. 1253–1263.

Negri, A., Villa, G., 2000. Calcareous nannofossil biostratigraphy, biochronology and paleoecology at the Tortonian/Messinian

boundary of the Faneromeni section (Crete). Palaeogeography, Palaeoclimatology, Palaeoecology 156, 195–209.

Nevesskaya, L.A., Goncharova, I.A., Il'ina, L.B., Paramonova, N.P., Khondkarian, S.O., 2003. The Neogene stratigraphic scale of the Eastern Paratethys. Stratigraphy and Geological Correlation 11 (2), 105–127.

Papp, A., Steininger, F.F., 1979. Paleogeographic implications of Late Miocene deposits in the Aegean region. Annales Géologiques des Pays Helléniques, Tome Hors Série 2, 955–959.

Pollak, W.H., 1979. Structural and lithological development of the Prinos–Kavala Basin, Sea of Thrace, Greece. Annales Géologiques des Pays Helléniques, Tome Hors Série 2, 1002–1011.

Popescu, S.-M., 2006. Late Miocene and early Pliocene environments in the southwestern Black Sea region from high-resolution palynology of DSDP Site 380A (Leg 42B). Palaeogeography, Palaeoclimatology, Palaeoecology, vol. 238, pp. 64–77. [this volume]. doi:10.1016/j.palaeo.2006.03.018.

Popov, S.V., Nevesskaya, L.A., 2000. Late Miocene brackish water mollusks and the history of the Aegean basin. Stratigraphy and Geological Correlation 8 (2), 195–205.

Proedrou, P., 1979. The evaporites formation in the Nestos–Prinos graben in the northern Aegean Sea. Annales Géologiques des Pays Helléniques, Tome Hors Série 2, 1013–1020.

Psilovikos, A., Syrides, G.E., 1983. Stratigraphy, sedimentation, and palaeogeography of the Strymon Basin, eastern Macedonia/northern Aegean Sea, Greece. Clausthaler Geologische Abhandlungen 44, 55–87.

Raffi, I., Rio, D., 1979. Calcareous nannofossil biostratigraphy of DSDP Site 132, Leg 13 (Tyrrhenian Sea, Western Mediterranean). Rivista Italiana di Paleontologia e Stratigrafia 85, 127–172.

Raffi, I., Backman, J., Rio, D., 1998. Evolutionary trends of tropical calcareous nannofossils in the Late Neogene. Marine Micropaleontology 35, 17–41.

Raffi, I., Mozzato, C., Fornaciari, E., Hilgen, F.J., Rio, D., 2003. Late Miocene calcareous nannofossil biostratigraphy and astrobiochronology for the Mediterranean region. Micropaleontology 49 (1), 1–26.

Rio, D., Raffi, I., Villa, G., 1990. Pliocene–Pleistocene calcareous nannofossil distribution patterns in the Western Mediterranean. Proceedings of the Ocean Drilling Program. Scientific Results 107, 513–533.

Rögl, F., Bernor, R.L., Dermitzakis, M.D., Müller, C., Stancheva, M., 1991. On the Pontian correlation in the Aegean (Aegina Island). Newsletters on Stratigraphy 24, 137–158.

Roveri, M., Bassetti, M.A., Ricci Lucchi, F., 2001. The Mediterranean Messinian salinity crisis: an Apennine foredeep perspective. Sedimentary Geology 140, 201–214.

Semenenko, V.N., Pevzner, M.A., 1979. Upper Miocene–Pliocene correlation of the Ponto-Caspian on biostratigraphic and paleomagnetic data. Izvestiya Akademii Nauk SSSR, Seriya. Geologicheskaya 9, 5–15.

Siesser, W.G., 1998. Calcareous nannofossil Genus *Scyphosphaera*: structure, taxonomy, biostratigraphy, and phylogeny. Micropaleontology 44 (4), 351–384.

Snel, E., Mărunțeanu, M., Macaleț, R., Meulenkamp, J.E., Van Vugt, N., 2006. Late Miocene to Early Pliocene chronostratigraphic framework for the Dacic Basin, Romania. Palaeogeography, Palaeoclimatology, Palaeoecology, vol. 238, pp. 107–124. [this volume]. doi:10.1016/j.palaeo.2006.03.021.

Steffens, P., Bruijn, H., Meulenkamp, J.E., Benda, L., 1979. Field guide to the Neogene of Northern Greece (Thessaloniki area and Strimon basin). Publications of the Department of Geology & Paleontology, University of Athens. Series A 35, 1–14.

Steininger, F.F., Papp, A., 1979. Current biostratigraphic and radiometric correlations of Late Miocene Central Paratethys stages (Sarmatian s.str., Pannonian s.str., and Pontian) and Mediterranean stages (Tortonian and Messinian) and the Messinian Event in the Paratethys. Newsletters on Stratigraphy 8 (2), 100–110.

Steininger, F.F., Berggren, W.A., Kent, D.V., Bernor, R.L., Sen, S., Agustí, J., 1996. Circum-Mediterranean Neogene (Miocene and Pliocene) marine–continental chronologic correlations of European mammal units. In: Bernor, R.L., Fahlbusch, V., Mittmann, H.-W. (Eds.), The Evolution of Western Eurasian Neogene Mammal Faunas. Columbia University Press, New York, pp. 7–46.

Stevanović, P.M., 1990. Rückschau auf pontische Stufe in Griechenland. In: Stevanović, P.M., Nevesskaja, L.A., Marinescu, F., Sokac, A., Jámbor, A. (Eds.), Pontien-Pl_1 (sensu F. Le Play, N.P. Barbot de Marny, N.I. Andrusov). Serie Chronostratigraphie und Neostratotypen, Neogen der Westlichen ("Zentrale") Paratethys 8. JAZU and SANU, Zagreb–Belgrade, pp. 340–352.

Syrides, G.E., 1998. Paratethyan mollusc faunas from the Neogene of Macedonia and Thrace, Northern Greece. Romanian Journal of Stratigraphy 78, 171–180.

Theodoridis, S., 1984. Calcareous nannofossil biozonation of the Miocene and revision of the Helicoliths and Discoasters. Utrecht Micropaleontological Bulletins 32, 1–272.

Van Couvering, J.A., Castradori, D., Cita, M.B., Hilgen, F.J., Rio, D., 2000. The base of the Zanclean Stage and of the Pliocene Series. Episodes 23 (3), 179–187.

Van der Zwaan, G.J., Jorissen, F.J., De Stigter, H.C., 1990. The depth dependency of planktonic/benthonic foraminiferal ratios: constraints and applications. Marine Geology 95, 1–16.

Van Hinsbergen, D.J.J., Kouwenhoven, T.J., Van der Zwaan, G.J., 2005. Paleobathymetry in the backstripping procedure: distinguishing between tectonic and climatic effects on depth estimates. Palaeogeography, Palaeoclimatology, Palaeoecology 221, 245–265.

Zijderveld, J.D.A., 1967. A.c. demagnetization of rocks: analysis of results. In: Collinson, D.W., Creer, K.M., Runcorn, S.K. (Eds.), Methods in Palaeomagnetism. Elsevier, Amsterdam, pp. 254–286.